ELPH workshop C033
「ハドロン分光に迫る反応と構造の物理」
2022年12月06-07日，仙台市

ハイパー核の反応計算による先端研究

原田　融
Toru Harada

大阪電通大共通教育/KEK理論センターJ-PARC分室
Osaka E.-C. Univ./KEK Theory Center, J-PARC Branch

Contents

1. Distorted-wave impulse approximation (DWIA)

J. Hufner et al, NPA234 (1974) 429.
E.H. Auerbach et al., Ann. Phys. (N.Y.) 148 (1983) 381.
C.B. Dover et al.,PRC22 (1980) 2073.

グリーン関数の方法　O.Morimatsu, K. Yazaki, NPA483 (1988) 493.

最適フェルミ平均　T. Harada, Y. Hirabayashi, NPA744 (2004) 323.

光学模型・チャネル結合法

Distorted-wave Impulse Approximation (DWIA)

J. Hufner et al, NPA234 (1974) 429.
E.H. Auerbach et al., Ann. Phys. (N.Y.) 148 (1983) 381.
C.B. Dover et al.,PRC22 (1980) 2073.

(π^+, K^+)

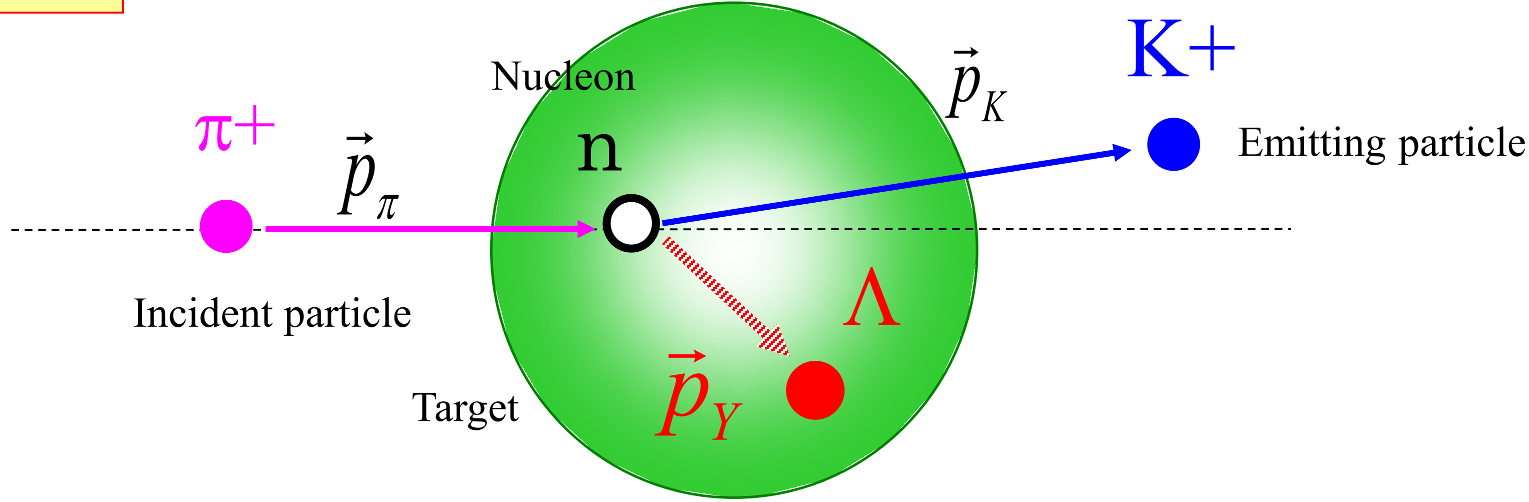

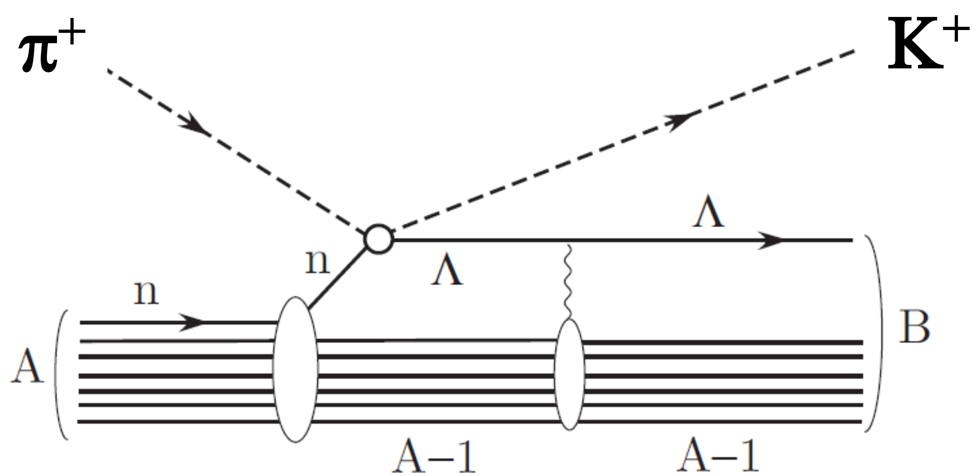

Distorted-wave Impulse Approximation (DWIA)

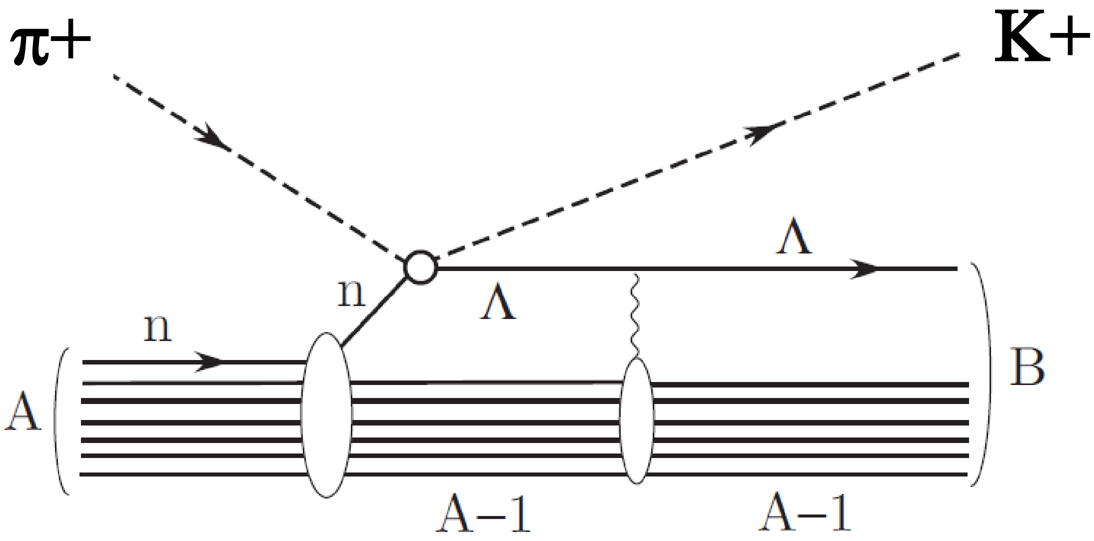

Energy and momentum transfer

$$\omega = E_\pi - E_K$$

$$\boldsymbol{q} = \boldsymbol{p}_\pi - \boldsymbol{p}_K$$

Inclusive differential cross section

$$\frac{d^2\sigma}{dE_K d\Omega_K} = \beta \frac{1}{[J_A]} \sum_{M_A} \sum_{B} |\langle \Psi_B | \hat{F} | \Psi_A \rangle|^2 \, \delta(E_K + E_B - E_\pi - E_A)$$

Production amplitude

$$\hat{F} = \int d\boldsymbol{r} \, \chi_K^{(-)*}(\boldsymbol{p}_K, \boldsymbol{r}) \chi_\pi^{(+)}(\boldsymbol{p}_\pi, \boldsymbol{r}) \sum_{j=1}^{A} \overline{f}_{\pi^+ n \to \Lambda K^+} \delta(\boldsymbol{r} - \boldsymbol{r}_j) \hat{O}_j$$

有効核子の方法（Effective number method）

Effective number

Differential cross section (closed shell targets Jp= 0+)

$$\left(\frac{d\sigma}{d\Omega}\right)_{\rm lab}^{J^\pi} = \alpha \left(\frac{d\sigma}{d\Omega}\right)_{\rm lab}^{\pi^+ n \to K^+ \Lambda} N_{\rm eff}^{J^\pi}(\theta)$$

Effective number of neutron

$$N_{\rm eff}^{J^\pi}(\theta) = \frac{1}{[J_A]} \sum_{m_B m_A} S_{j_n} \left| \langle (n\ell m)_n | \chi_K^{(-)*}(\boldsymbol{r}) \chi_\pi^{(+)}(\boldsymbol{r}) | (n\ell m)_\Lambda \rangle \right|^2$$

Kinematical factor

$$\alpha = \beta \left(1 + \frac{E_b}{E_B} \frac{p_b - p_a \cos\theta_{\rm lab}}{p_b}\right)^{-1}$$

運動学因子
（2体系から多体系への変換に伴う）

$$\beta = \left(1 + \frac{E_b^{(0)}}{E_Y^{(0)}} \frac{p_b^{(0)} - p_a \cos\theta_{\rm lab}}{p_b^{(0)}}\right) \frac{p_b E_b}{p_b^{(0)} E_b^{(0)}}$$

グリーン関数の方法 (Green's function method)

Green's function

Double-differential cross sections

$$\left(\frac{d^2\sigma}{dE_b\,d\Omega_b}\right) = \beta\left(\frac{d\sigma}{d\Omega_b}\right)^{aN\to bY}_{\text{lab}} S(E)$$

Morimatsu, Yazaki, NPA483 (1988) 493.

束縛状態・連続状態

Strength functions

$$\begin{aligned} S(E_B) &= \sum_B |\langle\Psi_B|\hat{F}|\Psi_A\rangle|^2 \delta(E_\pi + E_B - E_K - E_A) \\ &= (-)\frac{1}{\pi}\mathrm{Im}\sum_{\alpha\alpha'}\int d\mathbf{R}d\mathbf{R}' F^\dagger_\alpha(\mathbf{R}) G_{\alpha\alpha'}(E_B;\mathbf{R},\mathbf{R}') F_{\alpha'}(\mathbf{R}') \end{aligned}$$

Green's function

$$\sum_B |\Psi_B\rangle\delta(E-E_B)\langle\Psi_B| = (-)\frac{1}{\pi}\,\mathrm{Im}\left[\frac{1}{E-H_B+i\epsilon}\right]$$

Completeness relation

$$G^{(+)}(E;\boldsymbol{r},\boldsymbol{r}') = \sum_n \frac{\varphi_n(\boldsymbol{r})(\tilde{\varphi}_n(\boldsymbol{r}'))^*}{E-E_n+i\epsilon} + \frac{2}{\pi}\int_0^\infty dk \frac{k^2 S(k) u(k,\boldsymbol{r})(\tilde{u}(k,\boldsymbol{r}'))^*}{E-E_k+i\epsilon}$$

bound states, quasibound states　　Continuum states, resonance states

Elementary cross sections of $\pi N \rightarrow K^+\Lambda$, $K^+\Sigma^-$ reactions

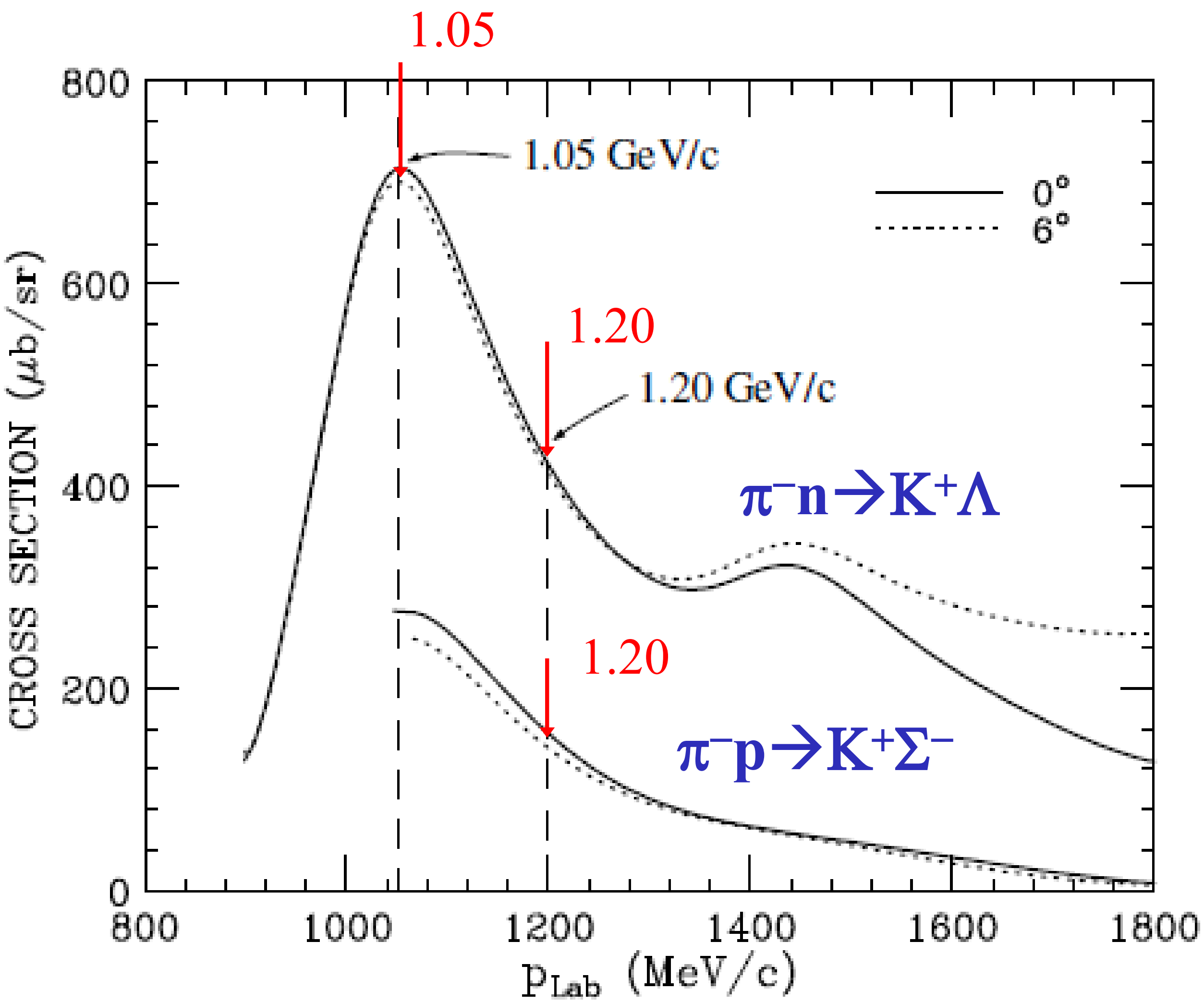

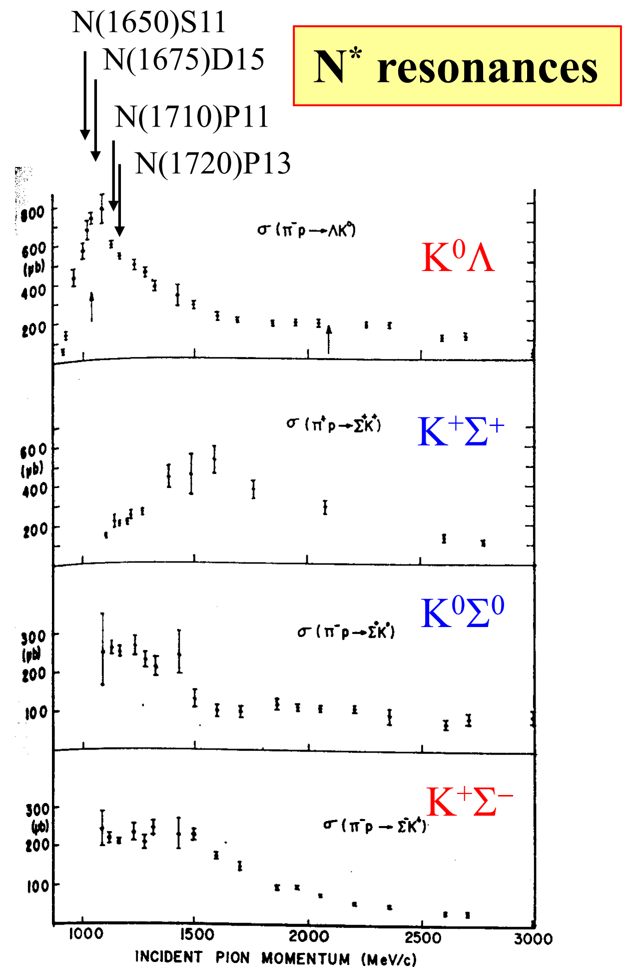

T.O.Binford, et al. PR183(1969)1134

⇨ There is a strong energy dependence of $(d\sigma/d\Omega)$.

Optimal Fermi-averaging (OFA) procedure 最適フェルミ平均

T. Harada and Y. Hirabayashi, NPA744 (2004) 323.

- ``Optimal'' cross section for π-p -> K+Σ⁻ reaction

$$\left(\frac{d\sigma}{d\Omega}\right)^{\rm opt} = \frac{p_K E_K}{(2\pi)^2 v_\pi} \left| t^{\rm opt}_{\pi N, K\Sigma}(p_\pi; \omega, \boldsymbol{q}) \right|^2$$

(π⁺, K⁺) reaction

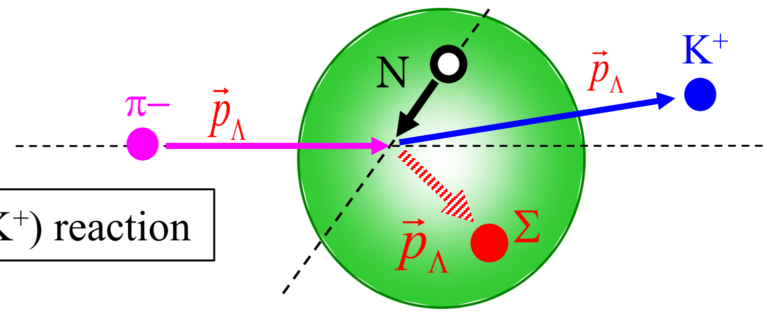

- Optimal Fermi-averaged πN -> KΣ *t*-matrix

$$\cos\theta_N = \hat{\boldsymbol{p}}_{\bar{K}} \cdot \hat{\boldsymbol{p}}_N$$

Elementary *t*-matrix

$$t^{\rm opt}_{\pi N, K\Sigma}(p_\pi; \omega, \boldsymbol{q}) = \left. \frac{\int_0^\pi \sin\theta_N \, d\theta_N \int_0^\infty dp_N \, p_N^2 \rho(p_N) t_{\pi N, K\Sigma}(E_{\pi N}; \boldsymbol{p}_\pi, \boldsymbol{p}_N)}{\int_0^\pi \sin\theta_N \, d\theta_N \int_0^\infty dp_N \, p_N^2 \rho(p_N)} \right|_{\boldsymbol{p}_N = \boldsymbol{p}_N^*}$$

momentum dist.

- On-energy-shell equation for a struck proton momentum: $\boldsymbol{p}_N^*$

$$\omega = \sqrt{(\boldsymbol{p}_N^* + \boldsymbol{q})^2 + m_\Sigma^2} - \sqrt{\boldsymbol{p}_N^{*2} + m_N^2}$$

including the binding effects.

Optimal momentum approximation (OMA):
S. A. Gurvitz, PRC33 (1986) 422.

$h = G_a^{-1} - G^{-1}$ vanishes

$$\tau = t_a + t_a G_a h G_a t_a + t_a G_a h (G_a + G_a t_a G_a) h G_a t_a + \cdots$$

Optimal cross section of the $\pi^+ n \rightarrow K^+ \Lambda$ reaction in nuclei

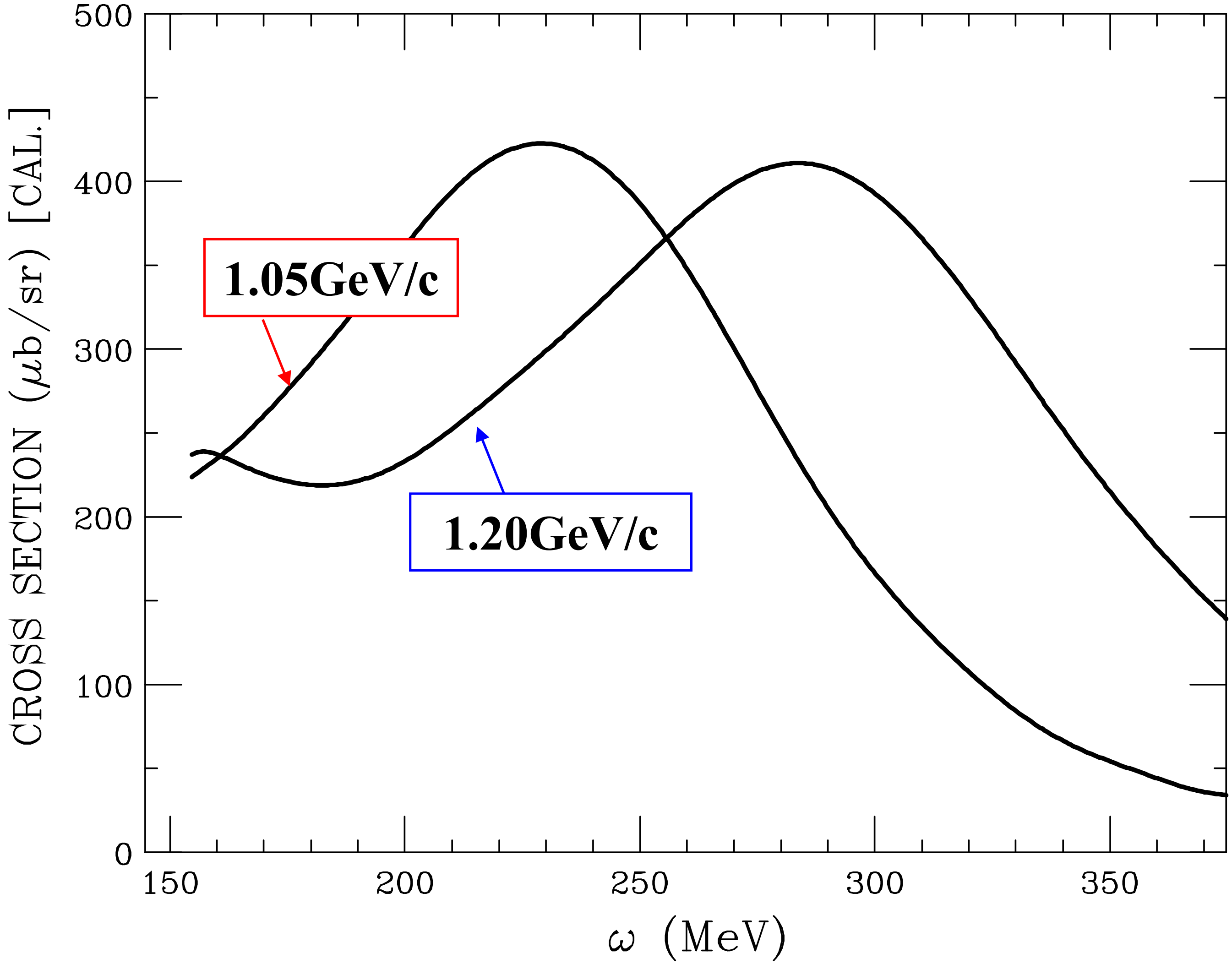

⇨ The ω dependence at 1.05 GeV/c are different from that 1.2GeV/c.

Application of Optimal Fermi-averaging (OFA) procedure

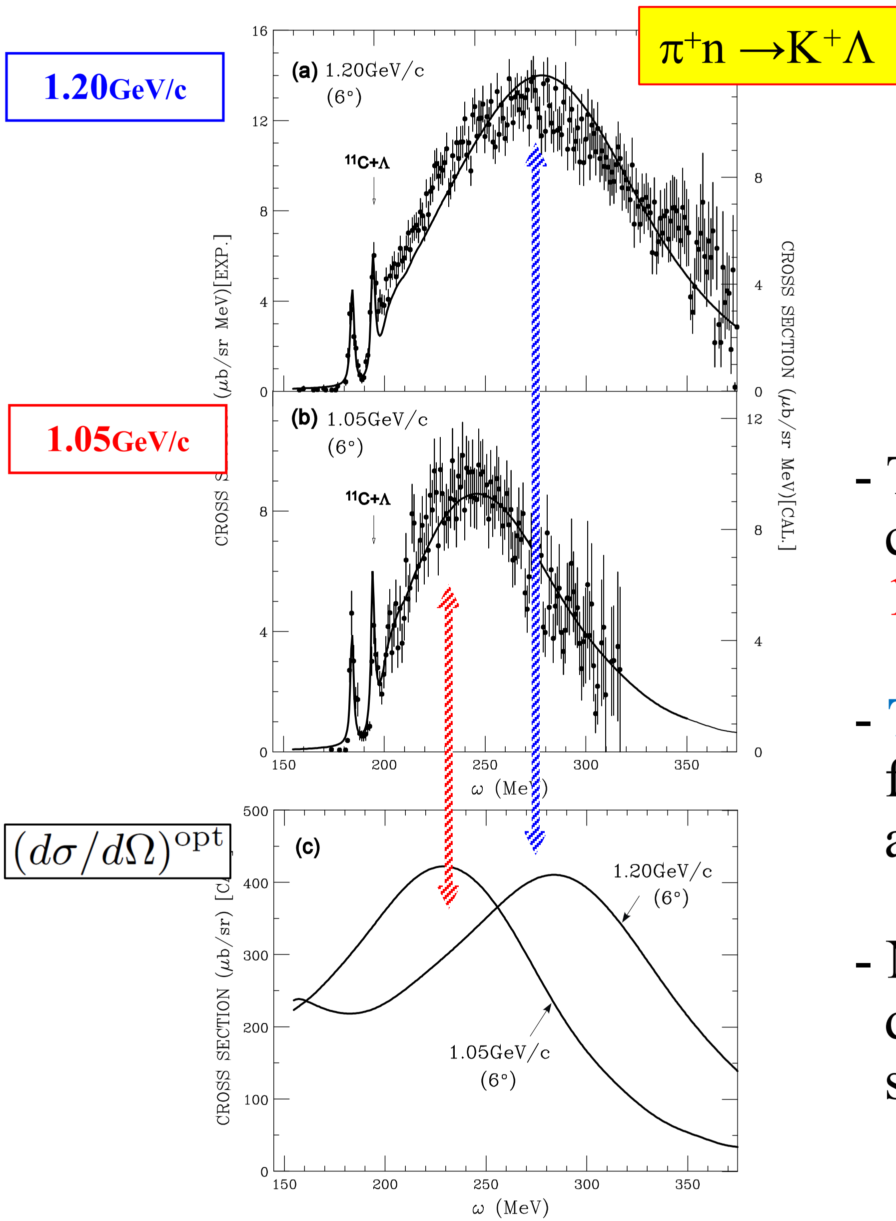

Λ production

^{12}C(π^+, K^+) reactions

- The calculated spectra in the QF region can explain the experimental data at 1.20GeV/c and 1.05GeV/c.

- **The ω energy-dependence** originates from the nature of the "optimal Fermi-averaging" t-matrix.

- Need careful consideration for energy-dependent of the elementary cross section.

Application of Optimal Fermi-averaging (OFA) procedure

^{28}Si(π^-,K$^+$)

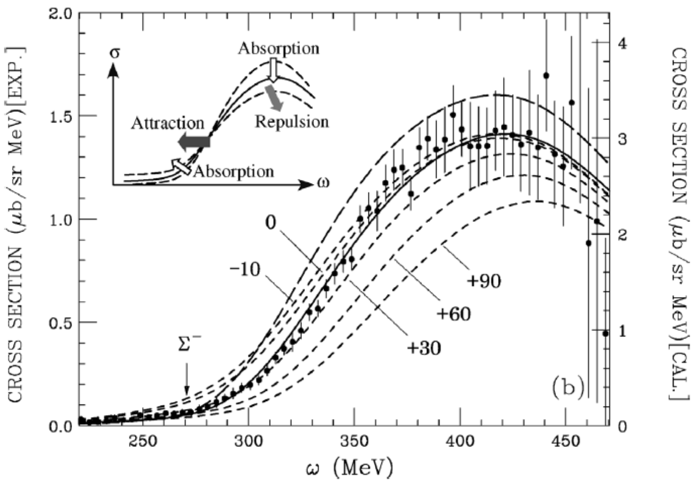

Σ^-

Harada, Hirabayashi, NPA759, 143 (2005).

^{209}Bi(π^-,K$^+$)

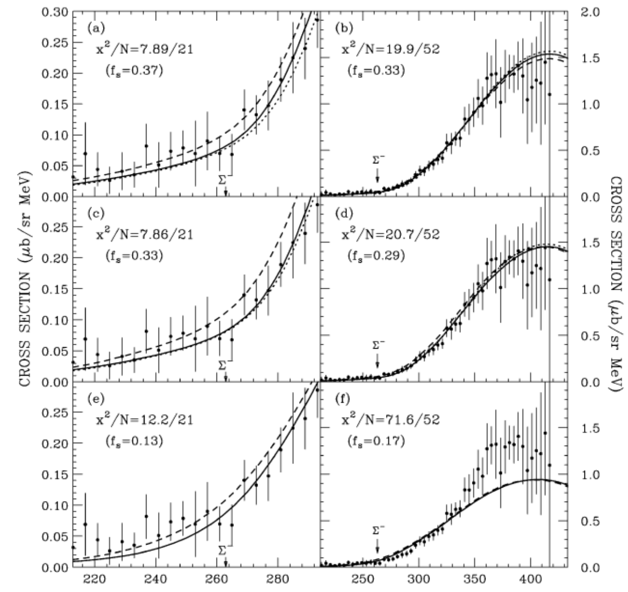

Σ^-

Harada, Hirabayashi, NPA767, 206 (2006).

^{6}Li(π^-,K$^+$)

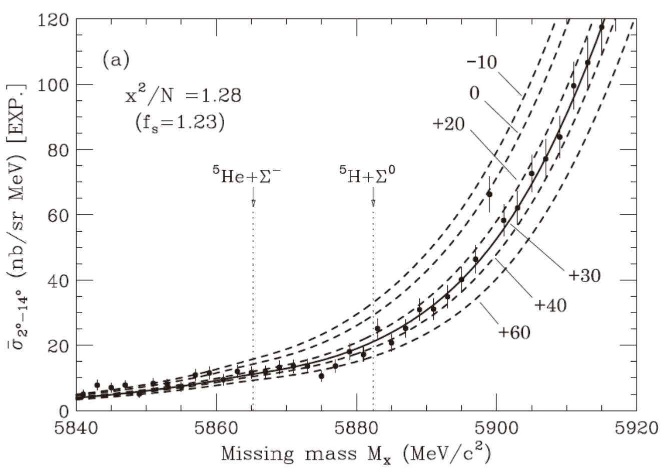

Σ^-

Harada, Honda, Hirabayashi, Phys. Rev. C 97, 024601 (2018).

^{9}Be(K$^-$,K$^+$)

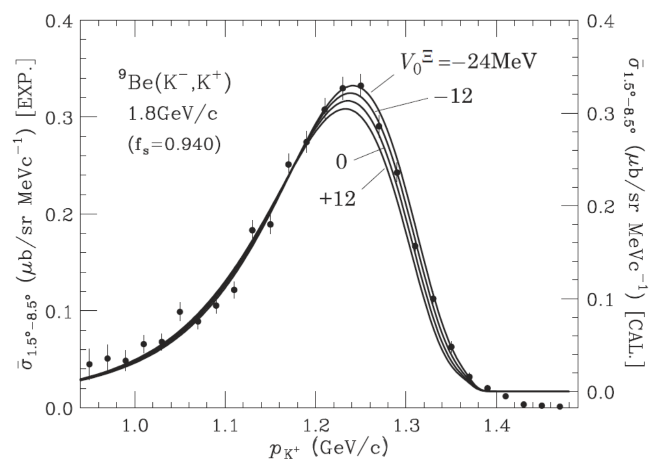

Ξ^-

Harada, Hirabayashi, PRC102 (2020) 024618.

Angular dependence of the optimal Fermi-av. cross section

"$\pi^- p \to K^+ \Sigma^-$ reactions" in the nucleus

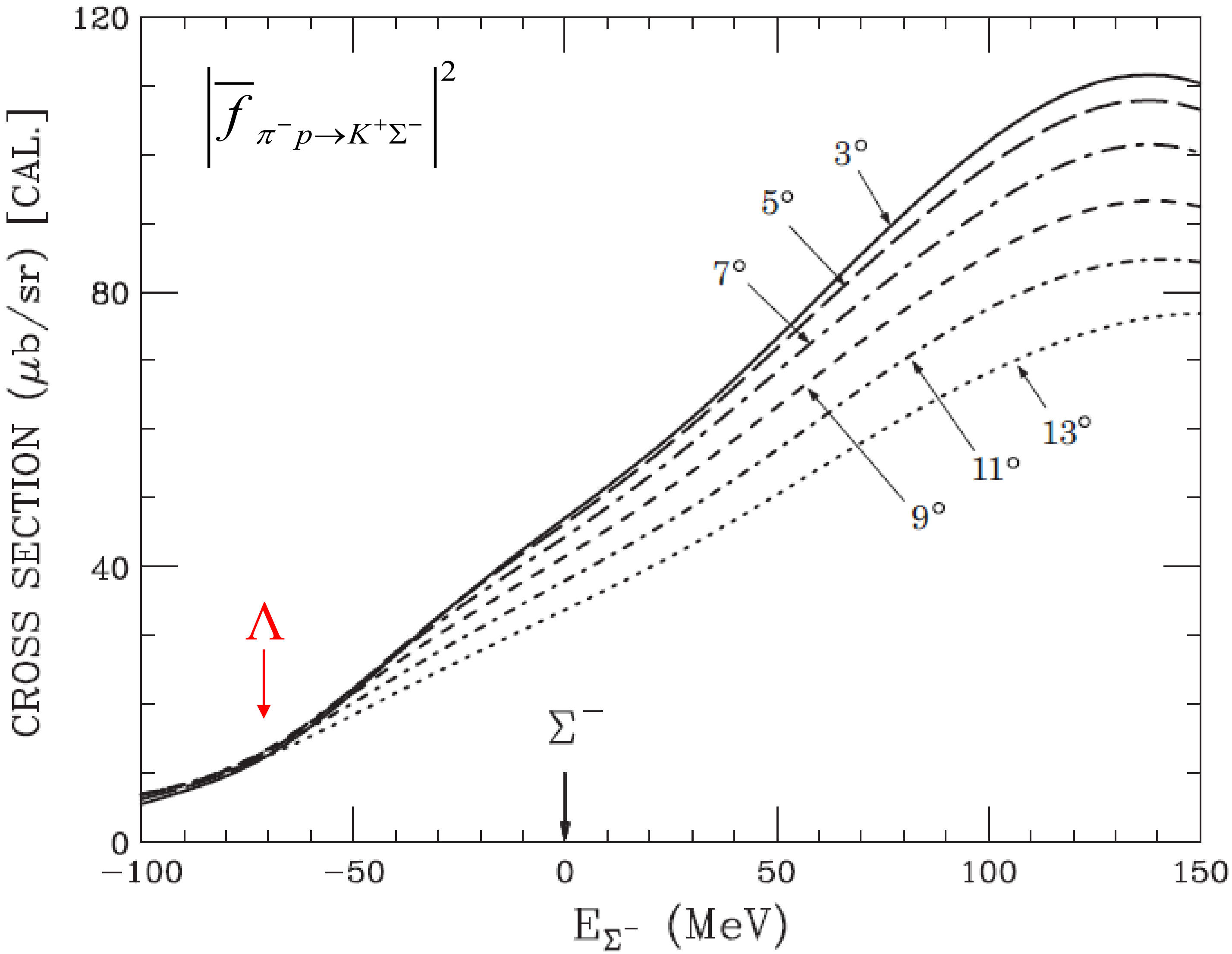

- There exists a strong energy dependence in the amplitudes.

Σ^--nucleus optical potentials for ^{27}Al, ^{57}Co, ^{207}Tl

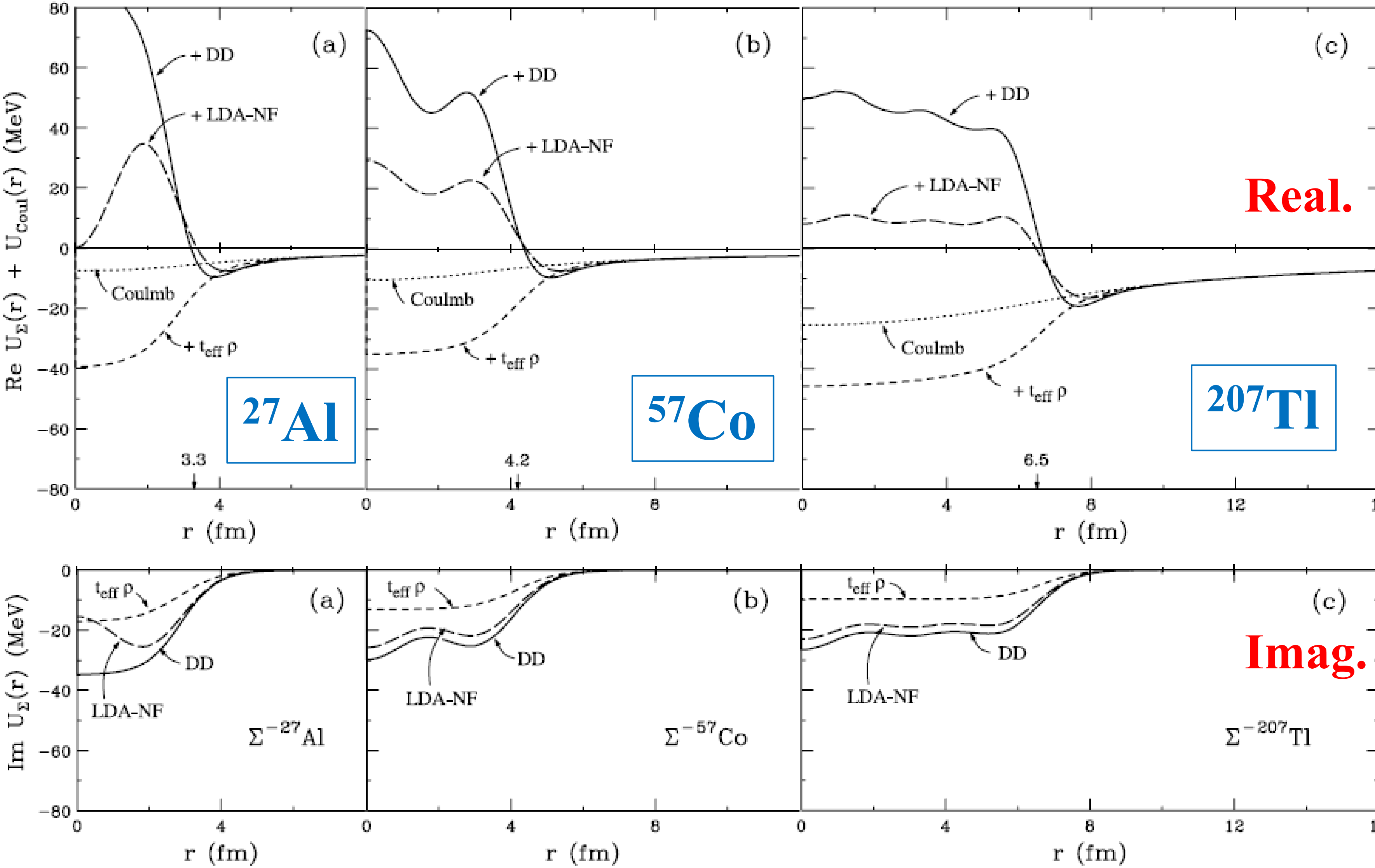

Fig. 2. (Top) Real and (bottom) imaginary parts of the Σ-nucleus potential plus the finite Coulomb potential for (a) Σ^-–^{27}Al, (b) Σ^-–^{57}Co and (c) Σ^-–^{207}Tl. The solid, long-dashed and dashed curves denote the radial distribution of the potentials for DD, LDA-NF and $t_{eff}\rho$, respectively. The strength for the real part includes the finite Coulomb potential. The dotted curves denote only the Coulomb potential for the Σ^--nucleus systems.

Dependnce of Σ^- spectrra in (π^-,K^+) reactions on (V_Σ,W_Σ)

$^{28}Si(\pi^-,K^+)$

T. Harada, Y. Hirabayashi, Nncl. Phys. A767 (2006)206.
[Data taken from P.K.Saha, H. Noumi, et al., PRC70(2004)044613]

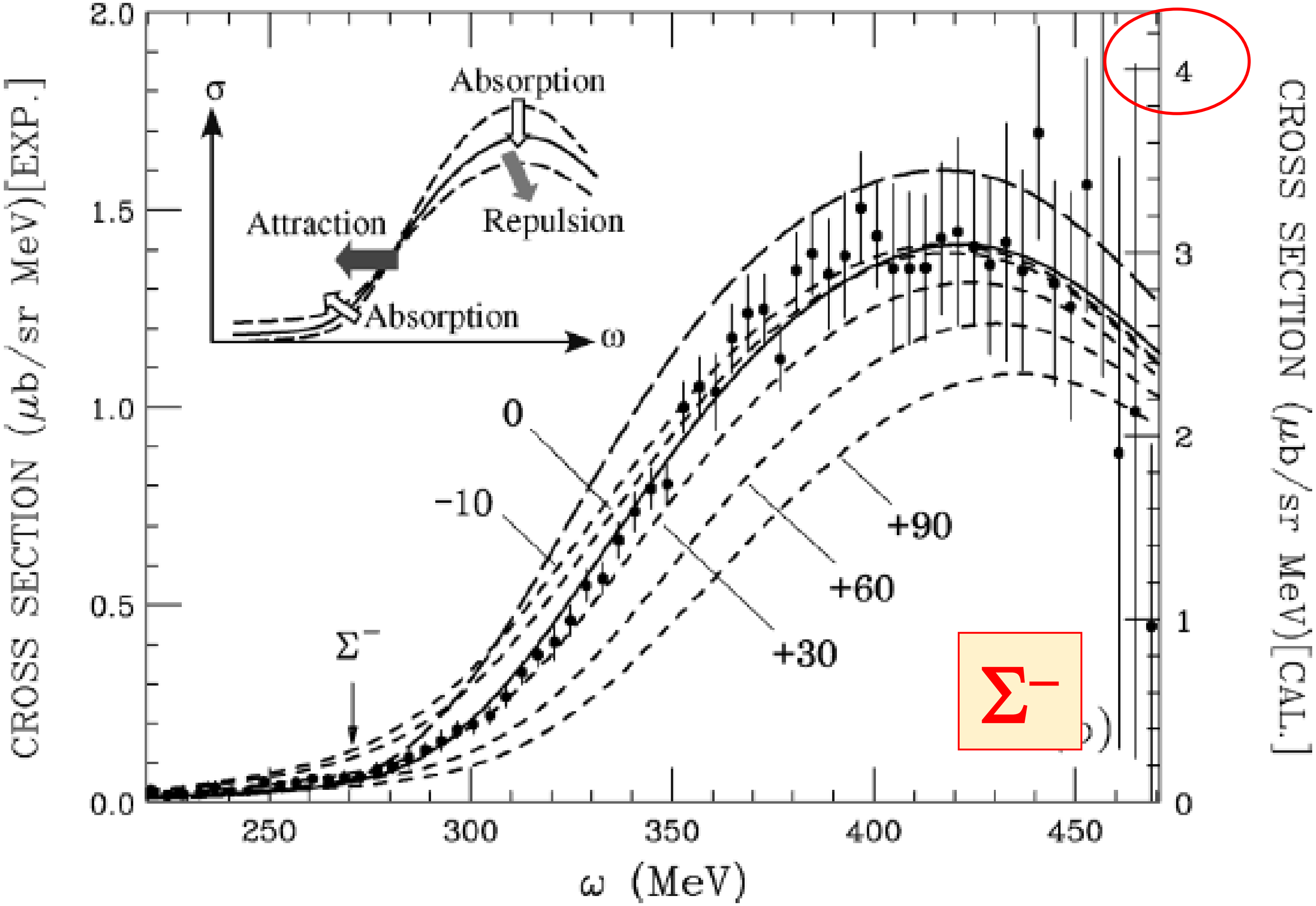

WS potential

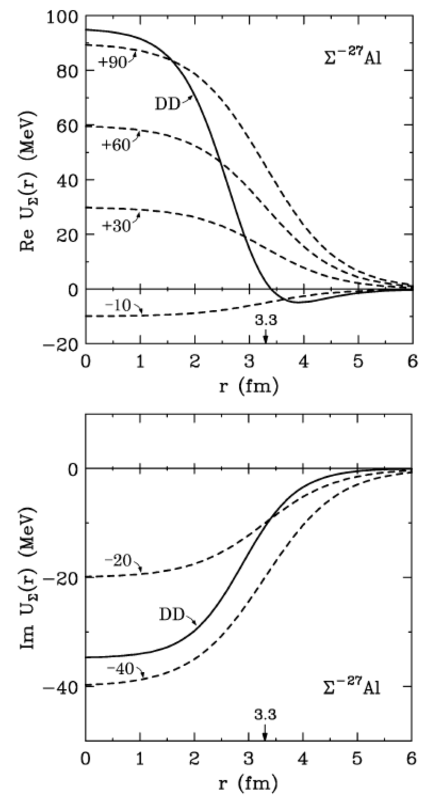

・引力的か斥力的かで、スペクトルの形が大きく異なる
・吸収の大きさによって、束縛領域のしみ出しの全体に対する割合が異なる。

Mass-number dependence of the integrated cross sections

Harada, Hirabayashi, NPA759 (2005) 143; NPA767 (2006) 206.

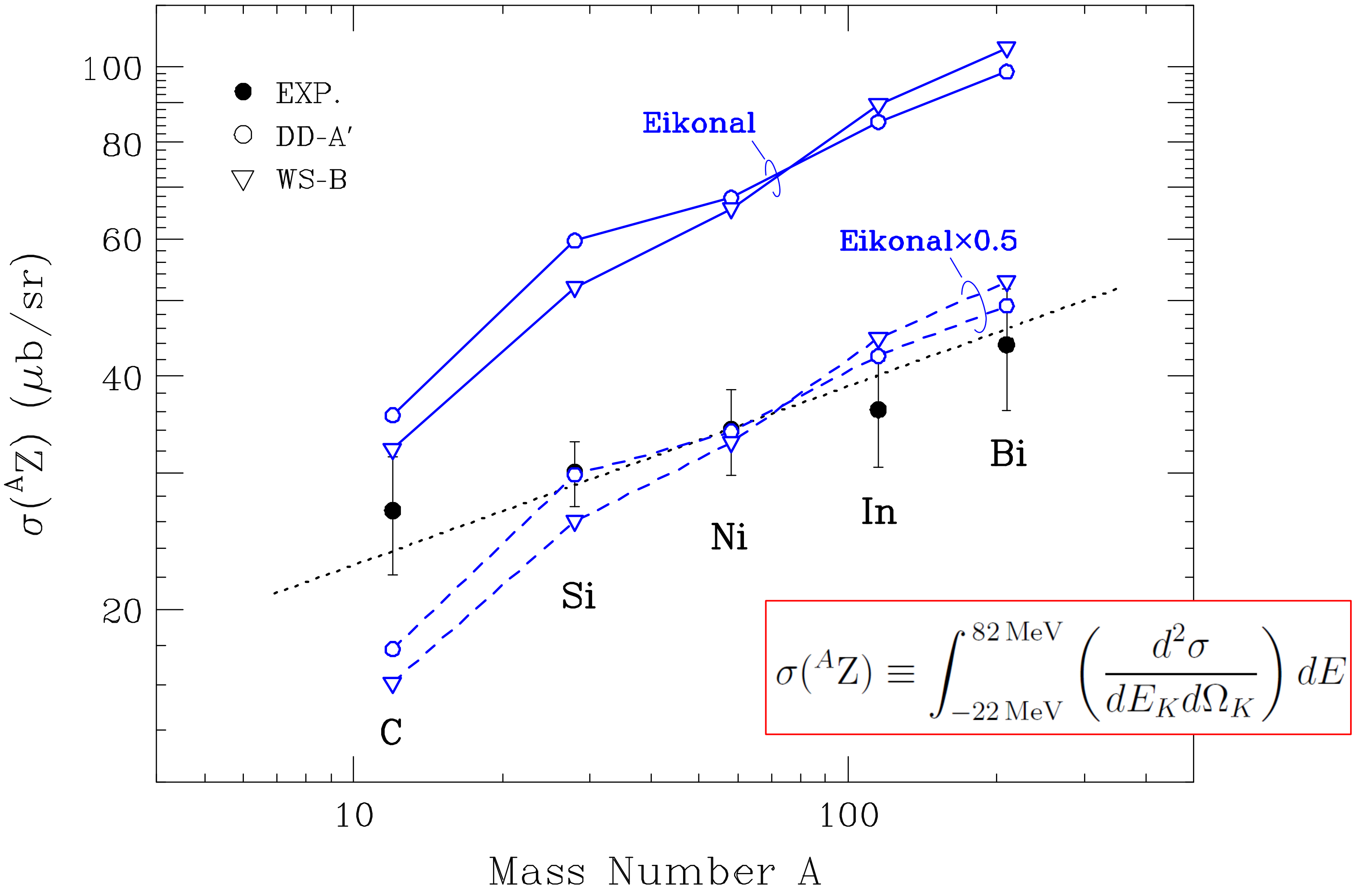

Angular distributions of π^-+^{12}C and K$^+$+ ^{12}C elastic reactions

Marlow et al., PRC 25 (1982) 2619.

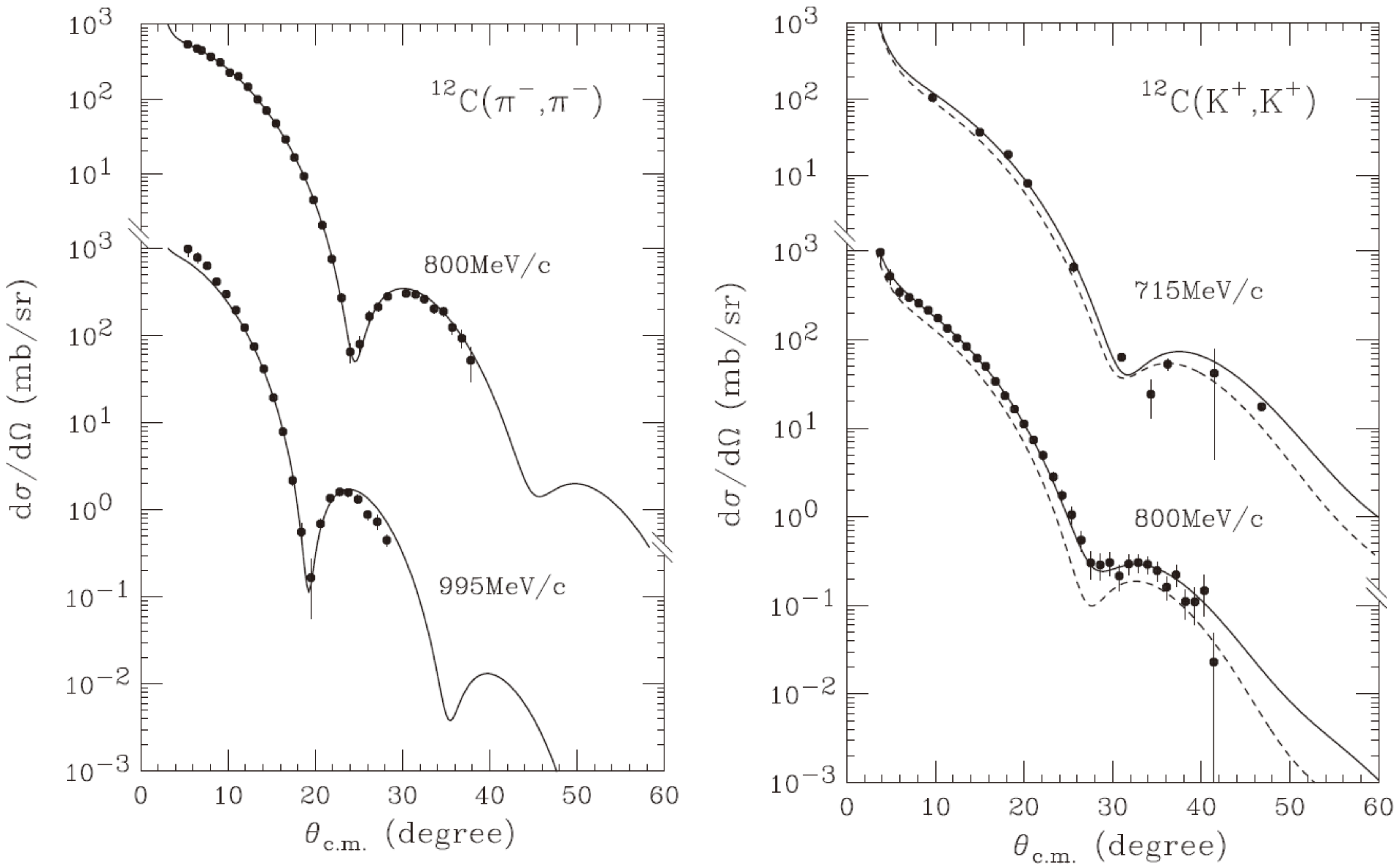

Σ^- spectrum by (π^-, K^+) reaction at 1.2GeV/c

T. Harada, Y. Hirabayashi, to be submitted (2022).

$^{28}Si(\pi^-,K^+)$

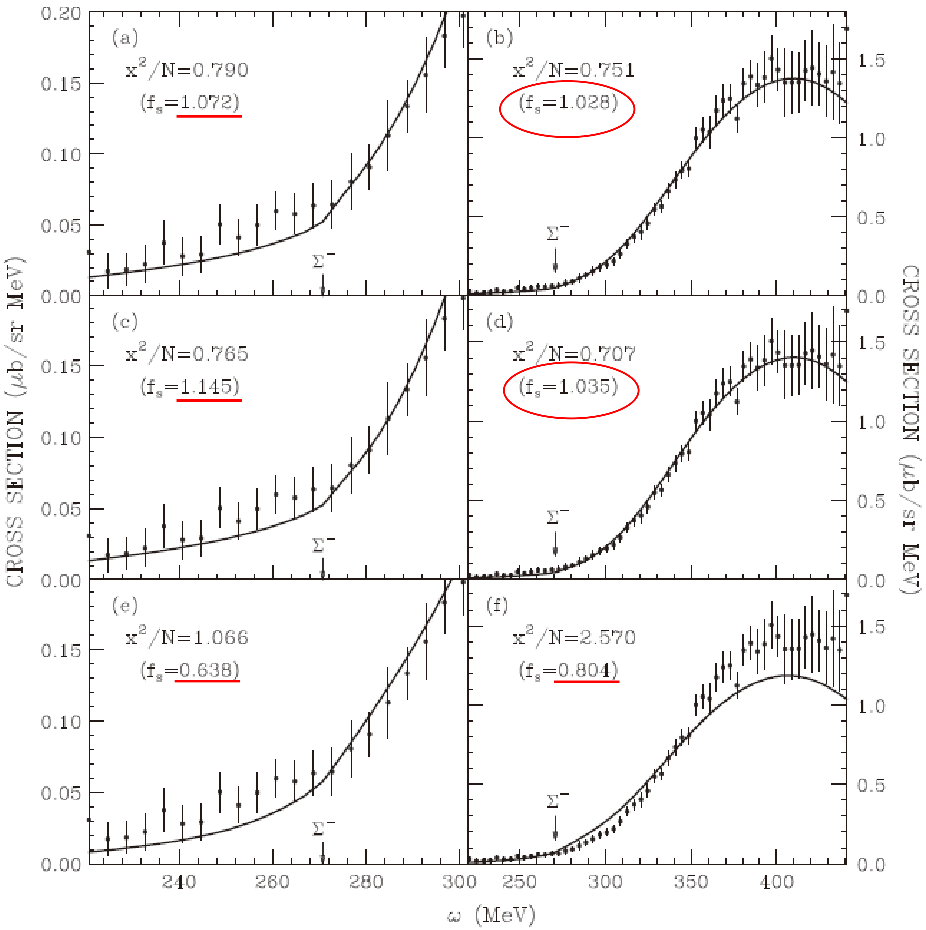

$^{209}Bi(\pi^-,K^+)$

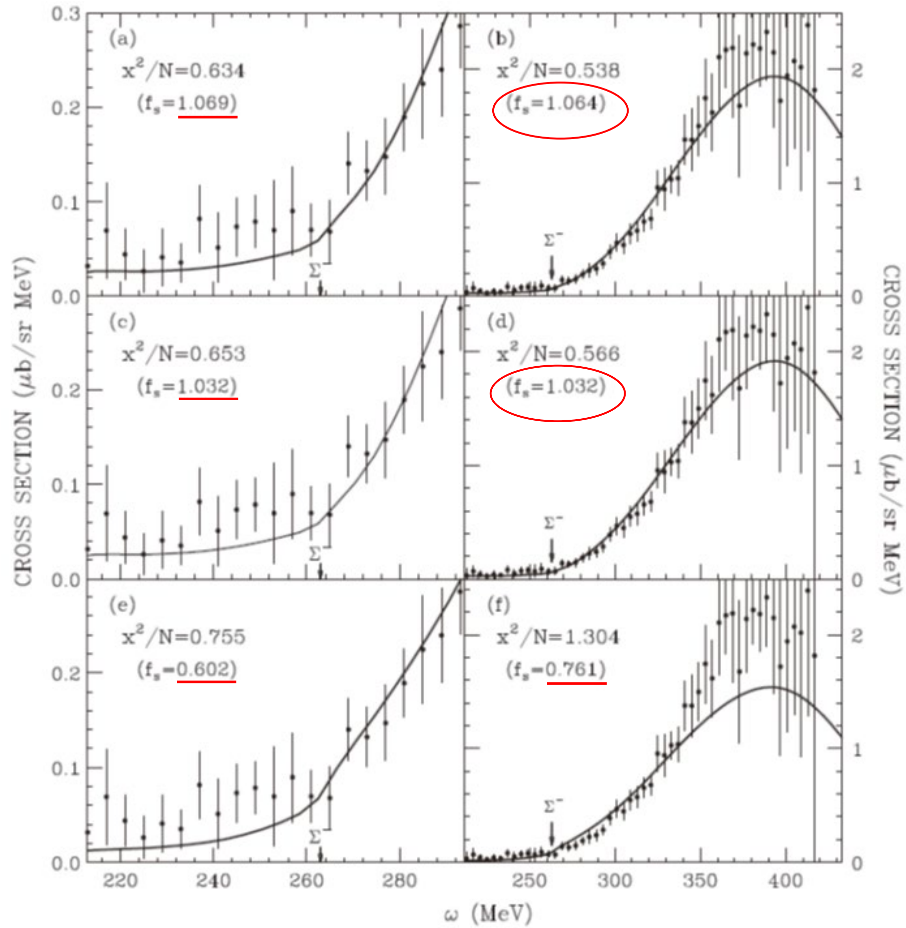

+ Distorted wave solving Klein-Gordon eq.
+ Absorption potential arising from $\Sigma N \to \Sigma N$ elastic scatterings

Mass-number dependence of the integrated cross sections

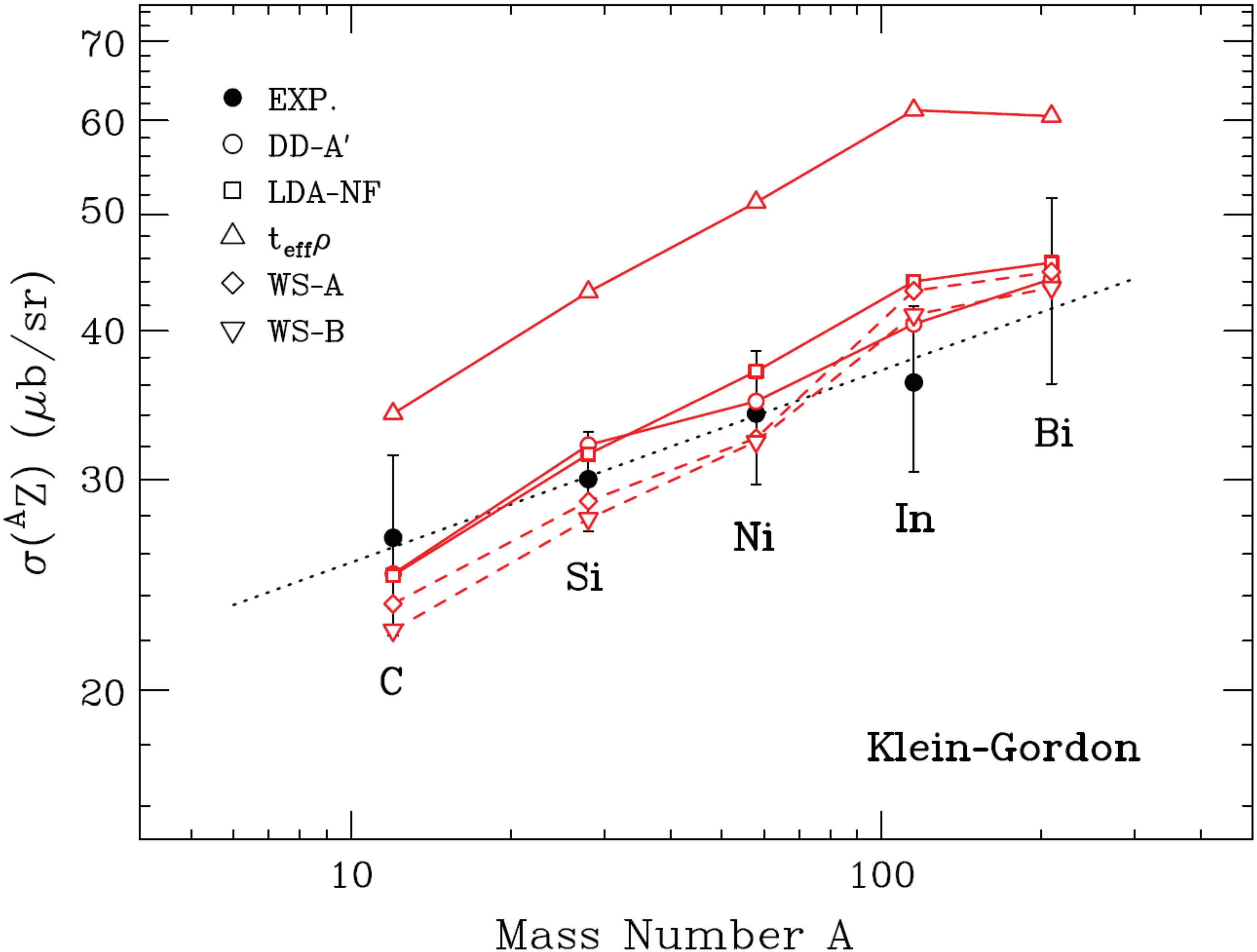

2. Ξ-nucleus potentials studied by (K^-, K^+) reactions

T. Harada, Y. Hirabayashi, PRC102 (2020) 024618.

T. Harada, Y. Hirabayashi, PRC103 (2021) 024605.

Study of the Ξ^--nucleus potential (1992-2010)

Emulsion @E173

point A : $\Xi^- + {}^{12}C \rightarrow {}^{4}_{\Lambda}H + {}^{9}_{\Lambda}Be$

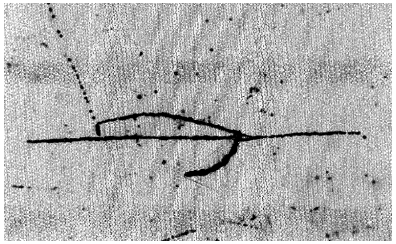

Y. Yamamoto, et al, PTP. Suppl. 117 (1994) 361.

$V_0^{\Xi} = -16$ MeV

DWIA analysis of ^{12}C(K-,K+) data at 1.8GeV/c

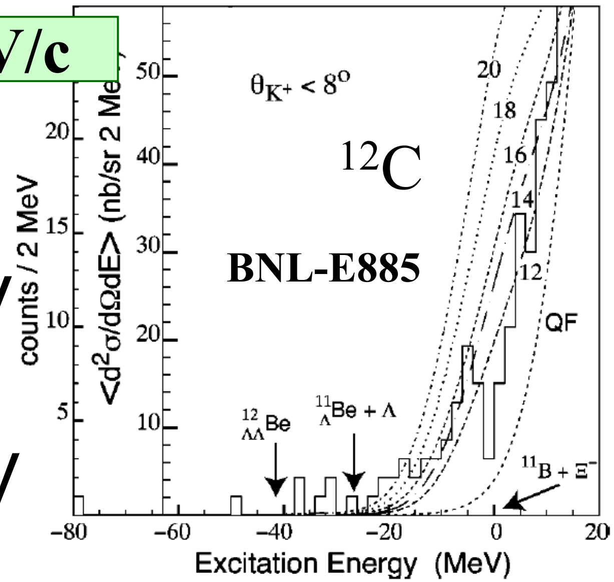

T.Iijima et al., NPA546(1992)588.

Tadokoro et al., PRC51(1995)2656.

$V_0^{\Xi} = -16$ MeV

P.Khaustov et al., PRC61(2000)054603.

$V_0^{\Xi} = -14$ MeV

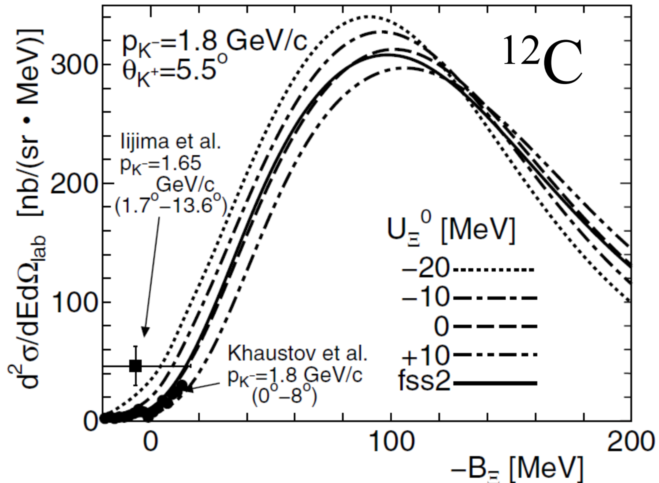

Semiclassical Distorted Wave Model

M. Kohno et al., PTP123(2010)157;

NPA835(2010)358.

$$V_\Xi^0 = -20, -10, 0, +10, +20 \text{MeV}$$

$\longleftrightarrow$ **fss2**

Recent observations of Ξ^- hypernuclei from emulsion compared with theoretical predictions

$\Xi^- + {}^{14}N$

M. Yoshimoto, Prog. Theor. Exp. Phys. **2021**, 073D02.

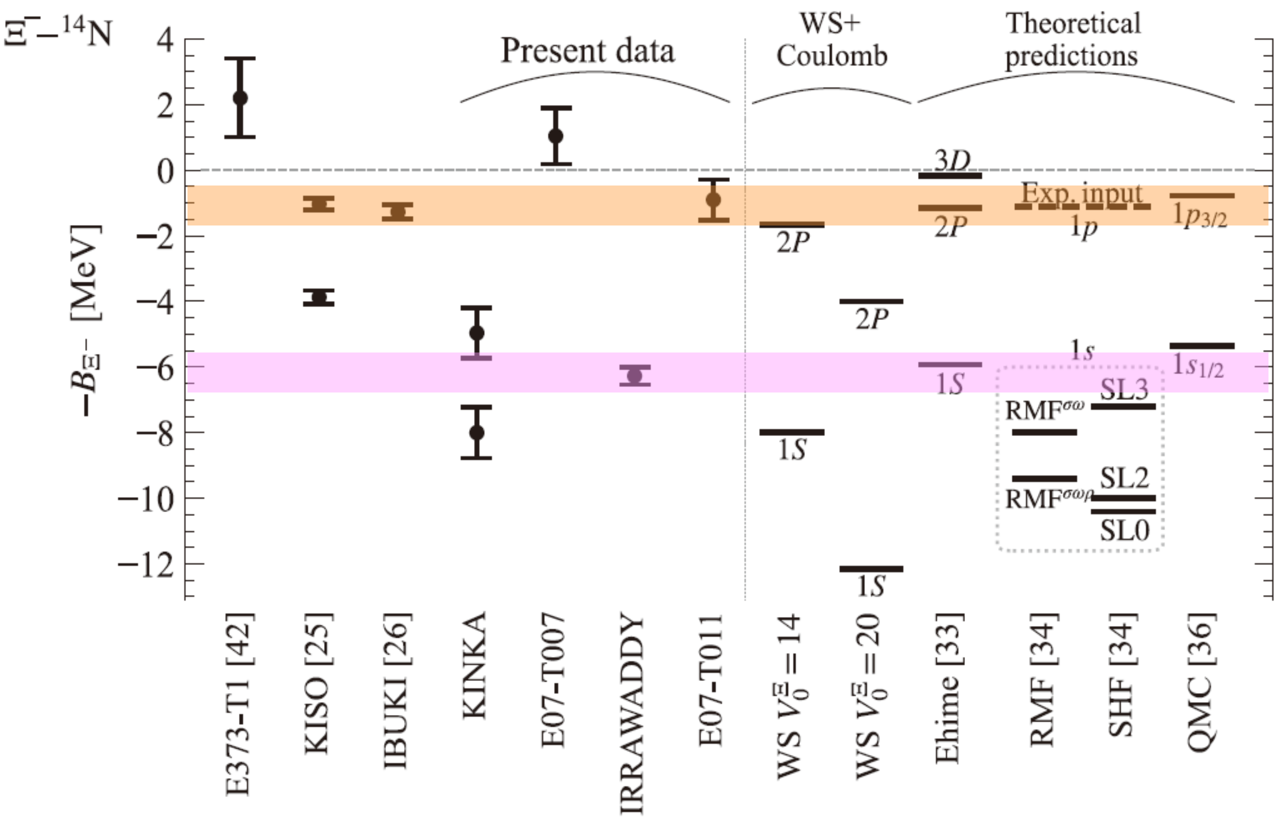

2P capture

1s?

Coulomb only in $\Xi^{-14}N$:
B_Ξ(2P)= 0.39 MeV
B_Ξ(1s)= 1.21 MeV

✓ Ξ^- capture from the 2P state: B_Ξ (2P) = 1.03 MeV(KISO)-1.27 MeV (IBUKI)

- The Ξ-nucleus potential is attractive in the real part.
- The 2P capture rate (4%) obtained from cascade cal.

→ ΞN-$\Lambda\Lambda$ coupling is weak (consistent with HAL-QCD).

Ξ^- QF spectra of the ^{9}Be(K$^-$, K$^+$) reaction at BNL-E906

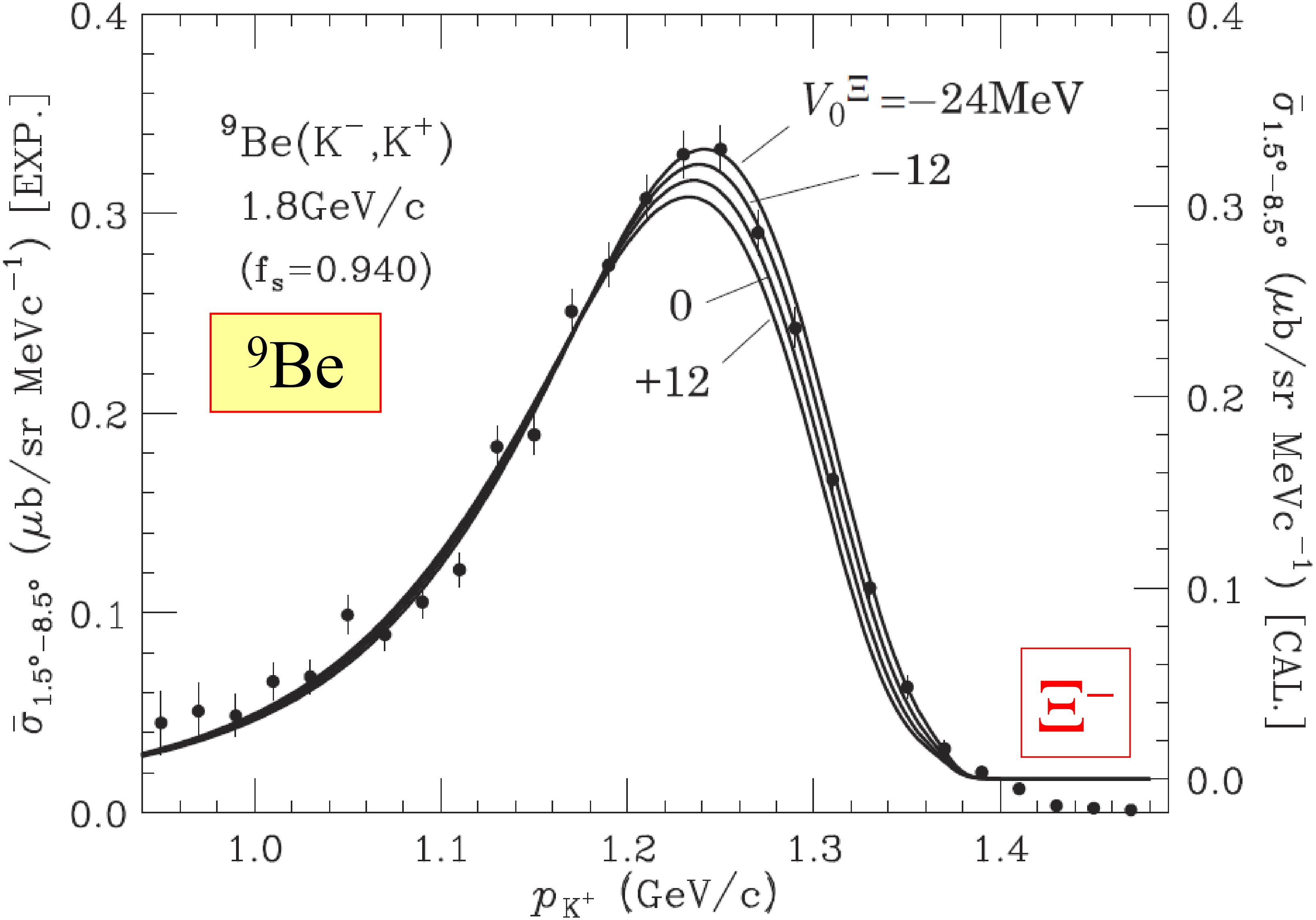

Contour plots of the χ^2-value distribution in $\{V_0, W_0\}$ plane

$$U_\Xi(r) = (V_0 + iW_0)/[1 + \exp\{(r - R)/a\}]$$

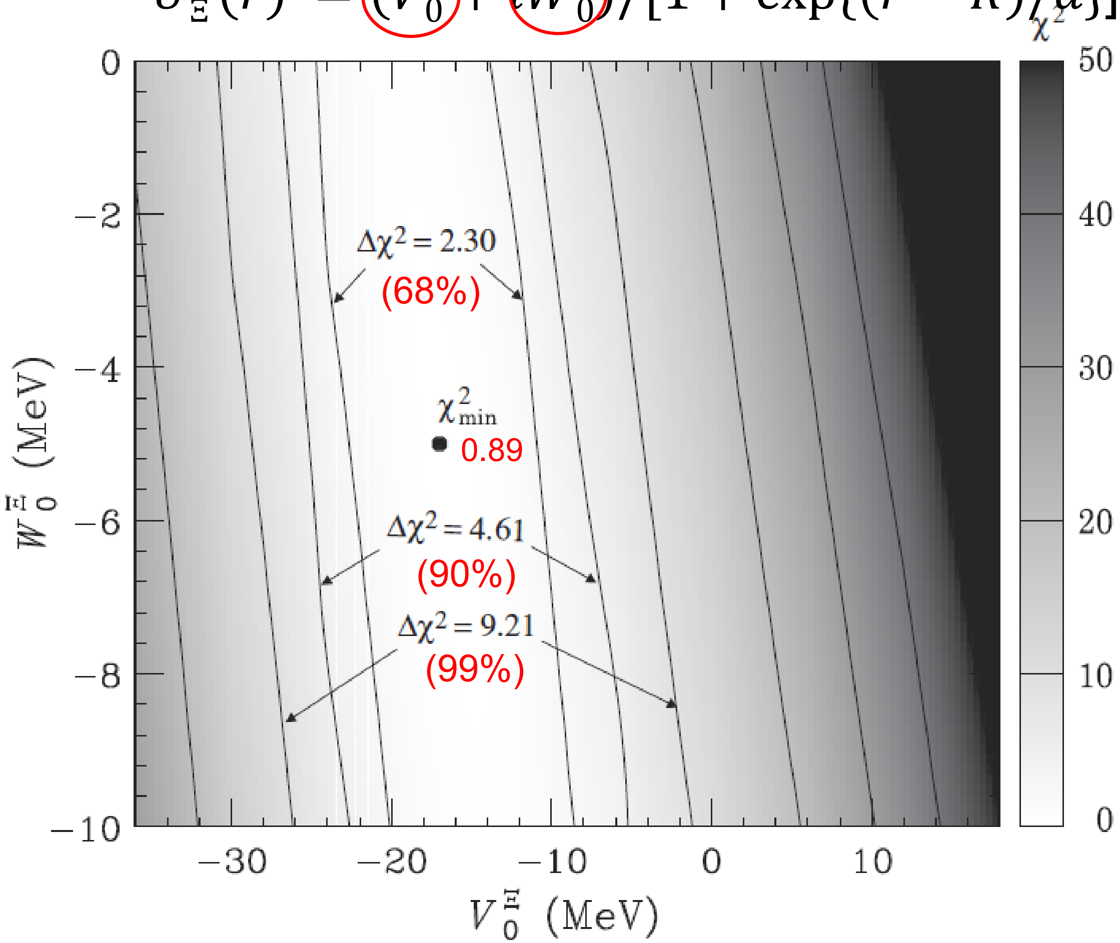

- ✓ The minimum position of $\chi^2_{min}/N = 15.2/17 = 0.89$, and $\Delta\chi^2 = 2.30$, 4.61, and 9.21 correspond to 68%, 90%, and 99% confidence levels for two parameters, respectively.
- ✓ The value of χ^2 is almost insensitive to W_0.

Remarks

- KEK-E224 and BNL-E885: **Fukuda et al., (1998)** **Khaustov et al. (2000)**
  $-V_0^{\Xi} = 14$ **MeV,** < 20 **MeV**
- BNL-E906:
  $-V_0^{\Xi} = 17 \pm 6$ **MeV** **Harada-Hirabayashi (2021)**
- Density dependence of $V_0^{\Xi}(\rho_0)$:
  $-V_0^{\Xi}(\rho_0) = 21.9 \pm 0.7$ **MeV** **Friedman-Gal (2021)**
- Microscopic calculations + ΞN G-matrix
  Lattice QCD, ChEFT: $-V_0^{\Xi} < 10$ **MeV**
  Ehime, NHD, NSC08, NSC16, …

→ Contributions of ΞN→ΛΛ coupling and ΞNN force?

weak (from HAL-QCD)

3. ${}^{3,4}_{\Lambda}H$ productions for ${}^{3}_{\Lambda}H$ lifetime puzzle

T. Harada, Y. Hirabayashi, NP1015 (2021) 122301.

$^{3}_{\Lambda}$H lifetime puzzle reported by high-energy heavy-ion collisions

Updated

ALICE (2020)	STAR (2022)	free Λ (PDG)
254 ± 15 ± 27 ps	221 ± 15 ± 29 ps	263±2 ps

THEIA-STRONG 2020 PRL128,202301 (2022)

Experimental plans of measurements of a $^{3}_{\Lambda}$H lifetime at J-PARC

J-PARC E74

Direct measurement of the $^{3}_{\Lambda}$H and $^{4}_{\Lambda}$H lifetimes using **^{3,4}He (π^-,K^0)$^{3,4}_{\Lambda}$H** reaction, *A. Feliciello et al.*

J-PARC E73

$^{3}_{\Lambda}$H and $^{4}_{\Lambda}$H mesonic weak decay lifetime measurement with **^{3,4}He (K^-,π^0)$^{3,4}_{\Lambda}$H** reaction, *Y. Ma et al.*

Phase-0 (June,2020): ^{4}He(K^-,π^0)$^{4}_{\Lambda}$H

Phase-1 (May,2021): ^{3}He(K^-,π^0)$^{3}_{\Lambda}$H

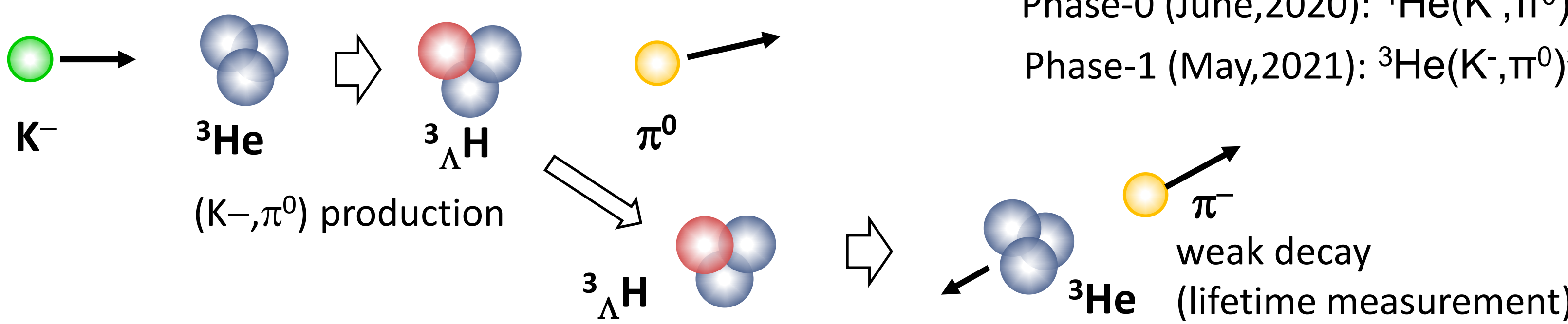

Theoretical calculations for the production cross sections

^{3,4}He(π+,K^+)$^{3,4}_{\Lambda}$He @1.05 GeV/c

T. Harada, unpublished (2006)

T. Harada, Y. Hirabayashi, PRC 100 (2019) 024605; JPS Conf. Proc., 17 (2017) 012008.

J-PARC E73

$^{3}_{\Lambda}H$ and $^{4}_{\Lambda}H$ mesonic weak decay lifetime measurement with **$^{3,4}He\ (K^-,\pi^0)^{3,4}_{\Lambda}H$** reaction, *Y. Ma et al.*

Pi− momentum distributions from $^{3}_{\Lambda}H$ and $^{4}_{\Lambda}H$ decays

Phase-0

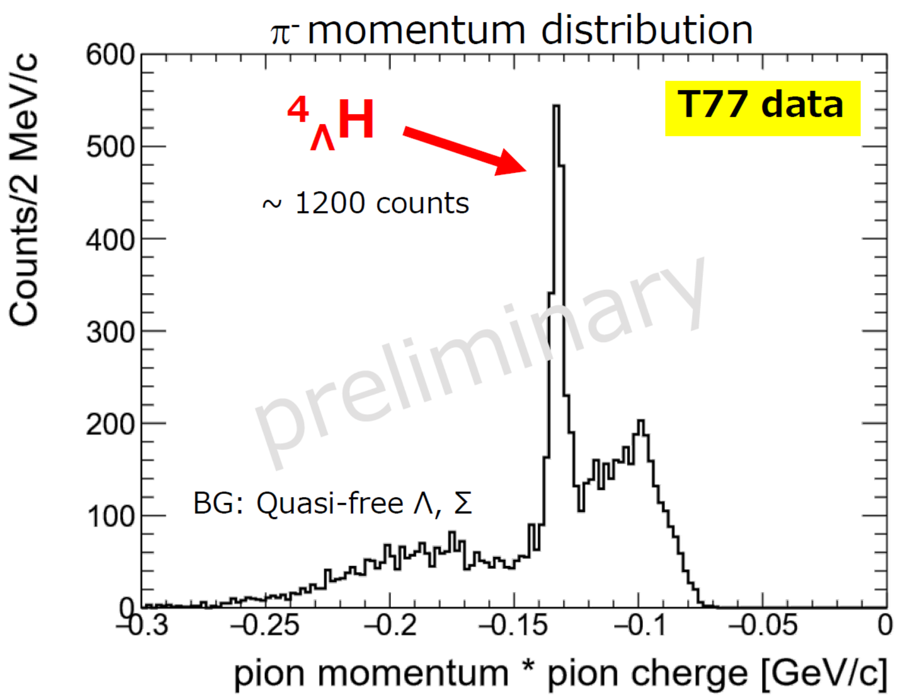

Phase-1

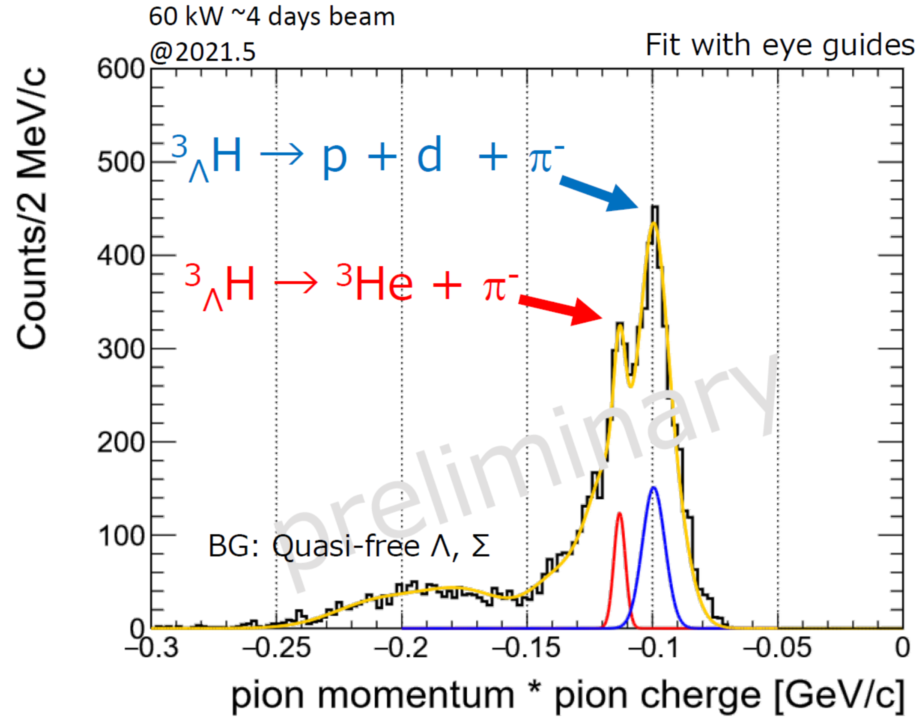

Data from the slide「J-PARCハドロン研究会2022」by Akaishi (Osaka Univ)

Relative density distributions for $^{3,4}_{\Lambda}H$ and $^{3,4}He$

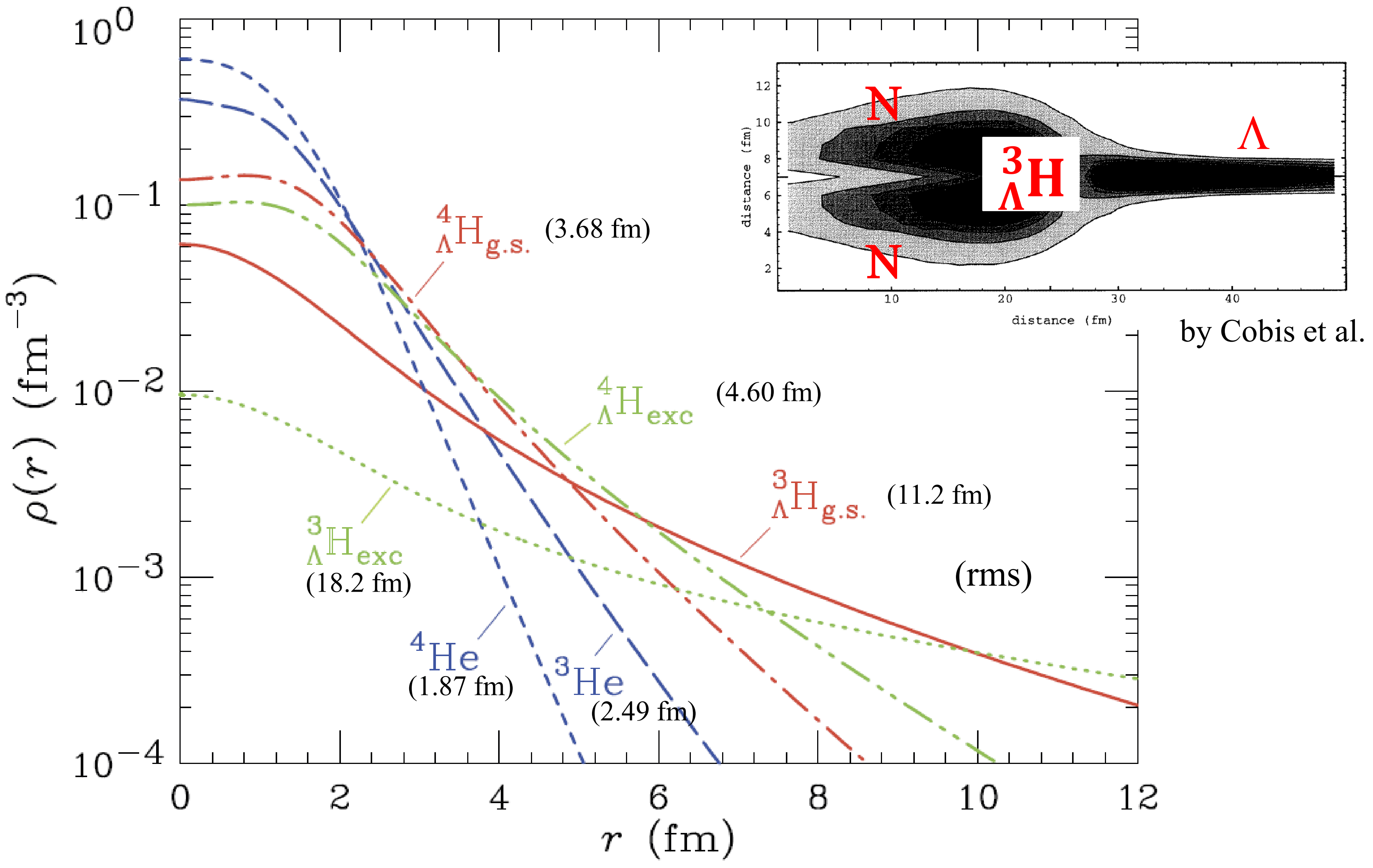

Comparison in production between $^{3}_{\Lambda}$H and $^{4}_{\Lambda}$H

To reduce uncertainties of several approximations and input parameters, we estimate $\hat{R}(\theta_{\rm lab}) = [d\sigma/d\Omega_{\rm lab}(^{3}_{\Lambda}{\rm H})]/[d\sigma/d\Omega_{\rm lab}(^{4}_{\Lambda}{\rm H})]$

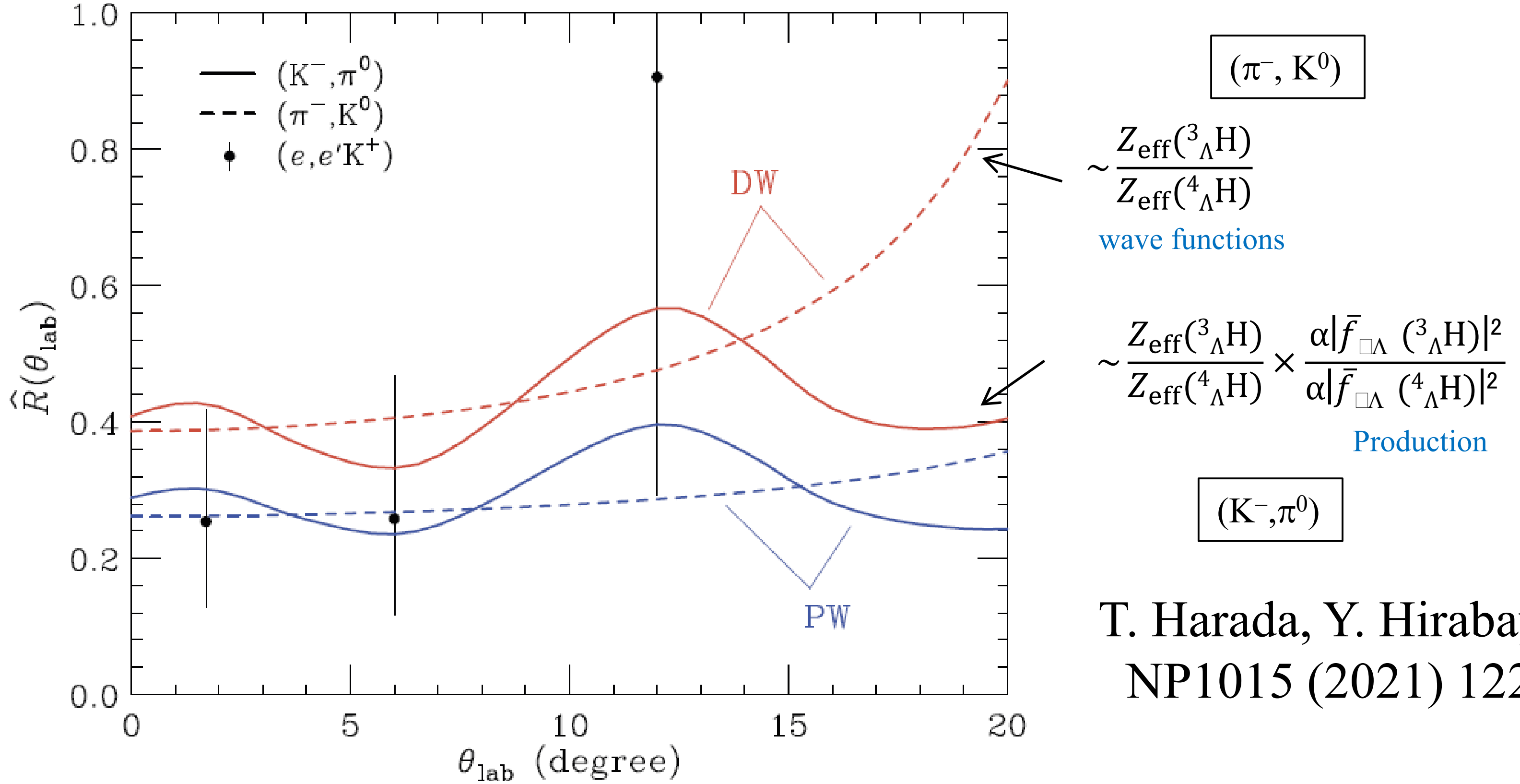

T. Harada, Y. Hirabayashi, NP1015 (2021) 122301.

R_{34} dependence on the $^{3}_{\Lambda}$H binding energy (Λ wave function)

$R_{34} \simeq 0.3 - 0.4$ (B_{Λ}=0.13MeV) Emulsion

$R_{34} \simeq 0.65$ (B_{Λ}=0.41MeV) STAR

J-PARC E73

$^{3}_{\Lambda}H$ and $^{4}_{\Lambda}H$ mesonic weak decay lifetime measurement with $^{3,4}He\ (K^{-},\pi^{0})^{3,4}_{\Lambda}H$ reaction, *Y. Ma et al.*

cross section ratio $^{3}_{\Lambda}H/\ ^{4}_{\Lambda}H$

- Rough estimation

	Hypernucleus	$^{4}_{\Lambda}H$	$^{3}_{\Lambda}H$	$^{3}_{\Lambda}H/^{4}_{\Lambda}H$	
Measured	# of Beam	5.04 G Kaon	8.84 G Kaon	1.75	Luminosity → 1 : 1.13 almost same
	# of target	0.145 g/cm^3 /4	0.070 g/cm^3 /3	0.64	
	# of signal	~1200	~200	0.15	
	Relative σ	1	0.3	R=0.3	

$R = \sigma_{lab}(^{3}_{\Lambda}H)/\sigma_{lab}(^{4}_{\Lambda}H)$

$R \sim 0.3$—0.4 @ $B_{\Lambda}=0.13$ MeV(Emulsion), ~ 0.65 @ $B_{\Lambda}=0.41$ MeV(STAR)

T. Harada and Y. Hirabayashi,
Nuclear Physics A 1015 (2021) 122301

→ **Binding energy does not seem to be large up to 0.41 MeV**

slide by Akaishi (Osaka Univ)

Remarks

- We have investigated theoretically productions of ${}^{3,4}_{\Lambda}$H bound states via ^{3,4}He(K^{-},π^{0}) reactions in the DWIA with the optimal Fermi-averaging K^{-}p→$\pi^{0}\Lambda$ t-matrix. We have calculated the differential cross sections dσ/dΩ and the integrated cross sections σ_{lab} in the ^{3,4}He(K^{-},π^{0}) reactions at 1.0 GeV/c and θ_{lab}=0°–20°.
- The comparison in dσ/dΩ_{lab} and σ_{lab} between ${}^{4}_{\Lambda}$H and ${}^{3}_{\Lambda}$H provides examining the mechanism of the production and structure of ${}^{3,4}_{\Lambda}$H in the (K^{-},π^{0}) reactions on ^{3,4}He at p_{K^-}=1.0 GeV/c;

$$R_{34} = \sigma_{lab}({}^{3}_{\Lambda}\mathrm{H})/\sigma_{lab}({}^{4}_{\Lambda}\mathrm{H}) \simeq 0.3 - 0.4$$

- This investigation confirms the feasibility of the lifetime measurements of ${}^{3}_{\Lambda}$H at the J-PARC experiments.

T. Harada and Y. Hirabayashi, NP1015 (2021) 122301.

4. Search for a ΣNN quasibound state

T. Harada, Y. Hirabayashi, PRC89, 054603 (2014)

Spectroscopic study of a possible Λnn and ΣNN resonances via the $(e, e'K^+)$ reaction with a ^{3}H target

B. Pandy et al., (Hall A Collaboration), PRC **105**, L051001 (**2022**).

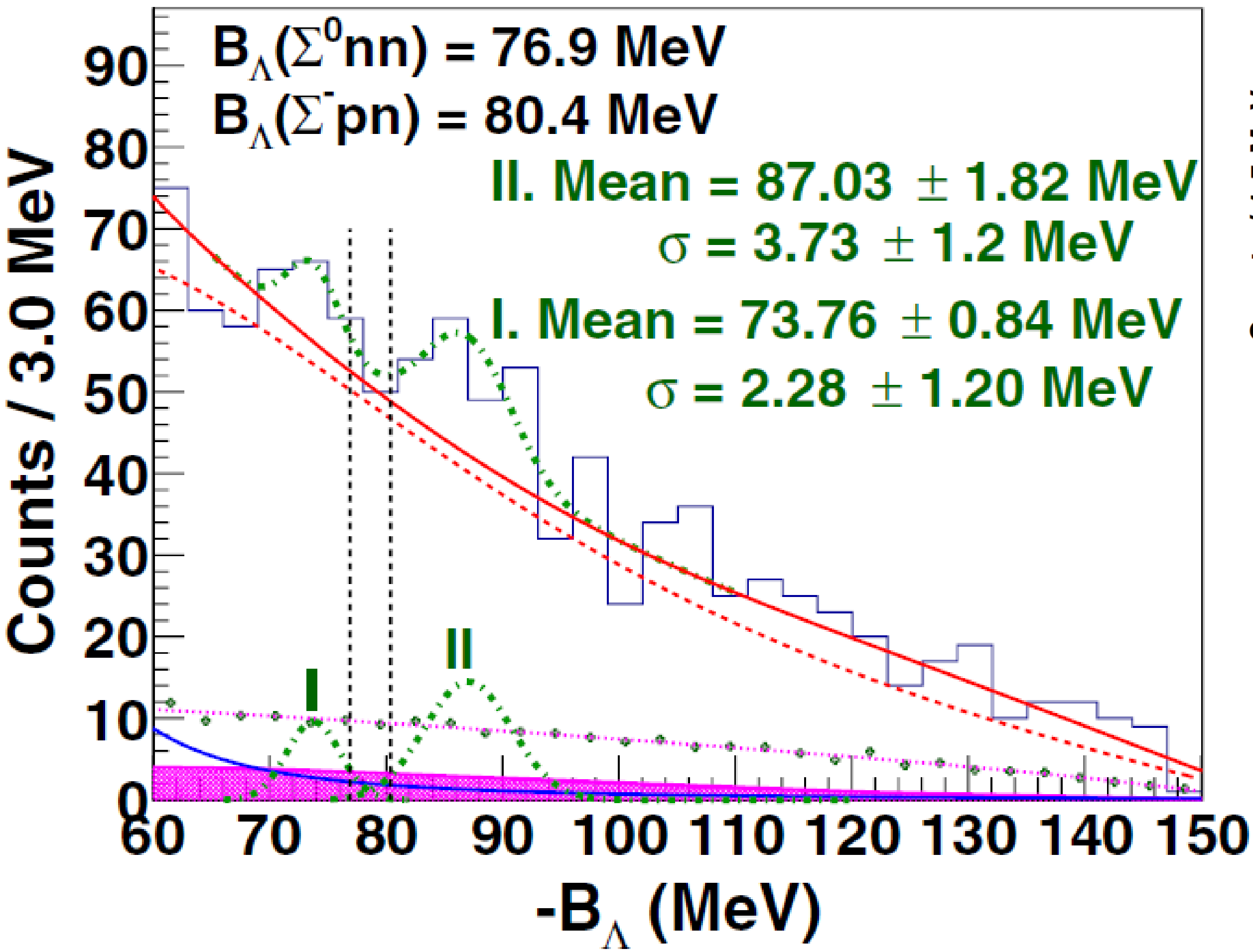

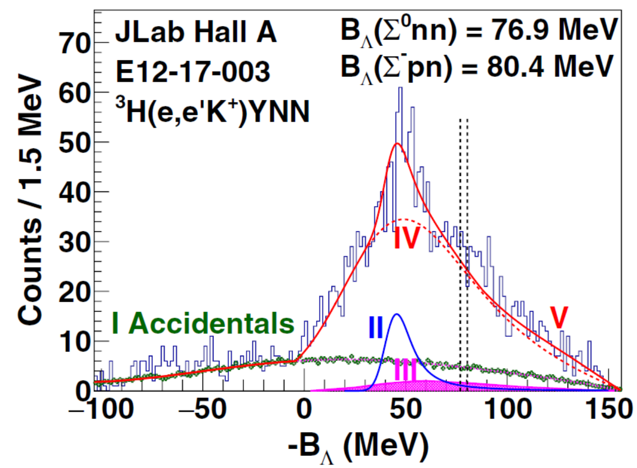

Historical background

- Faddeev calculation for ΣNN found a near-threshold $T = 0$ resonance in Λd elastic scattering. I. R. Afnan, B. F. Gibson, PRC **47**, 1000 (**1993**).
  B.F. Gibson, HYP2022 talk for $T = 1$ resonance
- Three-body variational calculations for ΣNN found a quasi bound state with $T = 1$, $S = 1/2$. Y. H. Koike, T. Harada, NPA **611**, 461 (**1996**).
- Faddeev calculation for ΣNN in a chiral constituent quark model found a near-threshold resonance with $T =1$, $S =1/2$.
  H. Garcilazo, et al., PRC **75**, 034002 (**2007**).
- Recently, the JLab ^{3}H$(e, e'K^+)\Sigma^0$nn experiment showed that these were interpreted as possible ΣNN resonances.
  B. Pandy et al., PRC **105**, L051001 (**2022**).

Our purpose

We study a search for a ΣNN quasibound state in the ^{3}He$(K^-, \pi^\mp)$ reactions theoretically.

T. Harada and Y. Hirabayshi, PRC **89**, 054603(2014).

Microscopic (2N)-Y folding-model potentials

T.Harada, Y.Hirabayashi, PRC89, 054603 (2014)

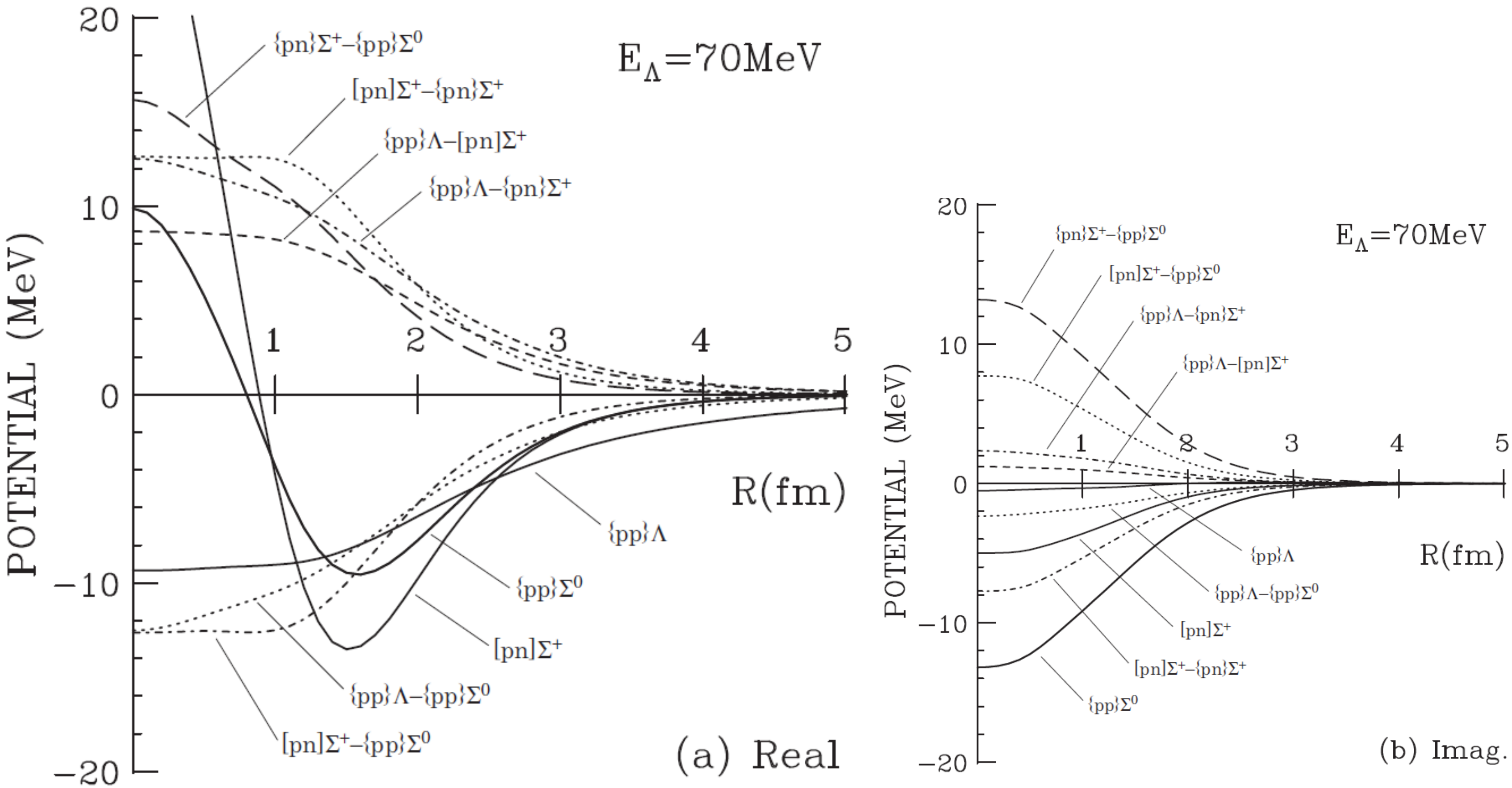

Coupled-channels DWIA calculation for Λ-Σ production

Coupled-channel Green's function

T.Harada, NPA672(2000)181

$$\hat{\mathbf{G}}(E_f) = \hat{\mathbf{G}}^{(0)}(E_f) + \hat{\mathbf{G}}^{(0)}(E_f)\hat{\mathbf{U}}\hat{\mathbf{G}}(E_f)$$

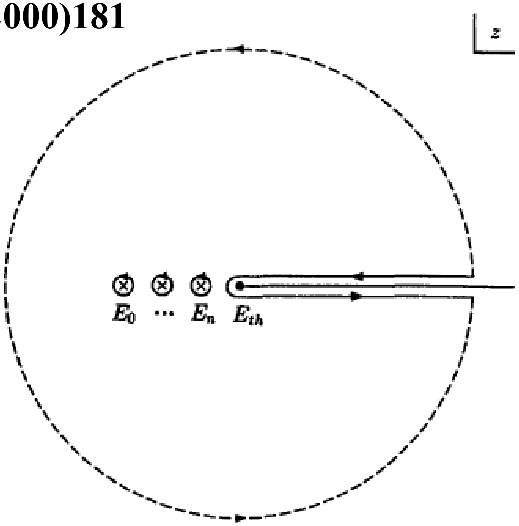

$$\hat{\mathbf{G}}^{(0)}(E_f) = \begin{bmatrix} G_\Lambda^{(0)} & & \\ & G_{\Sigma^+}^{(0)} & \\ & & G_{\Sigma^0}^{(0)} \end{bmatrix} \quad \hat{\mathbf{U}} = \begin{bmatrix} U_{\Lambda,1/2} & U_{X,1/2} & 0 \\ U_{X,1/2} & U_{\Sigma,1/2} & 0 \\ 0 & 0 & U_{\Sigma,3/2} \end{bmatrix}$$

$$\mathrm{Im}\,\hat{G} = \underbrace{\hat{\Omega}^{(-)\dagger}\{\mathrm{Im}\,\hat{G}_\Lambda^{(0)}\}\hat{\Omega}^{(-)}}_{\Lambda\text{ escape}} + \underbrace{\hat{\Omega}^{(-)\dagger}\{\mathrm{Im}\,\hat{G}_{\Sigma^+}^{(0)}\}\hat{\Omega}^{(-)}}_{\Sigma^+\text{ escape}} + \underbrace{\hat{\Omega}^{(-)\dagger}\{\mathrm{Im}\,\hat{G}_{\Sigma^0}^{(0)}\}\hat{\Omega}^{(-)}}_{\Sigma^0\text{ escape}} + \underbrace{\hat{G}^\dagger\{W_{Y,T}\}\hat{G}}_{\text{Spreading (2N breakup)}}$$

Strength function

Green's function method

Morimatsu, Yazaki, NPA483(1988)493

$$S(E_B) = \sum_B |\langle\Psi_B|\hat{F}|\Psi_A\rangle|^2\delta(E_\pi + E_B - E_K - E_A)$$

$$= (-)\frac{1}{\pi}\mathrm{Im}\sum_{\alpha\alpha'}\int d\mathbf{R}d\mathbf{R}' F_\alpha^\dagger(\mathbf{R})G_{\alpha\alpha'}(E_B;\mathbf{R},\mathbf{R}')F_{\alpha'}(\mathbf{R}')$$

Green's function

Poles of the S-matrix

Single channel

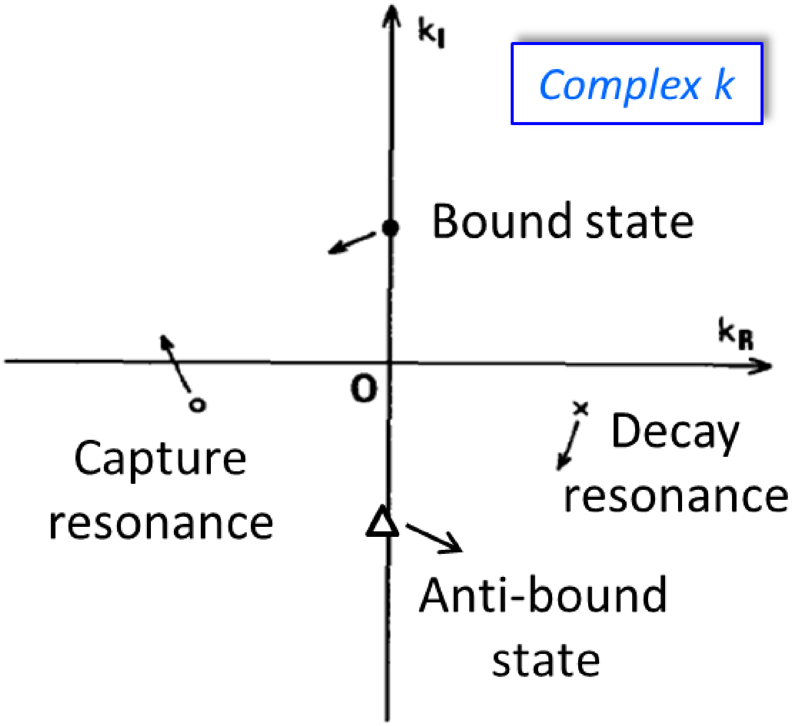

By Morimatsu-Yazaki

$$E_n = \frac{(k_n^{(\mathrm{pole})})^2}{2\mu} = -B_n - i\frac{\Gamma_n}{2}$$

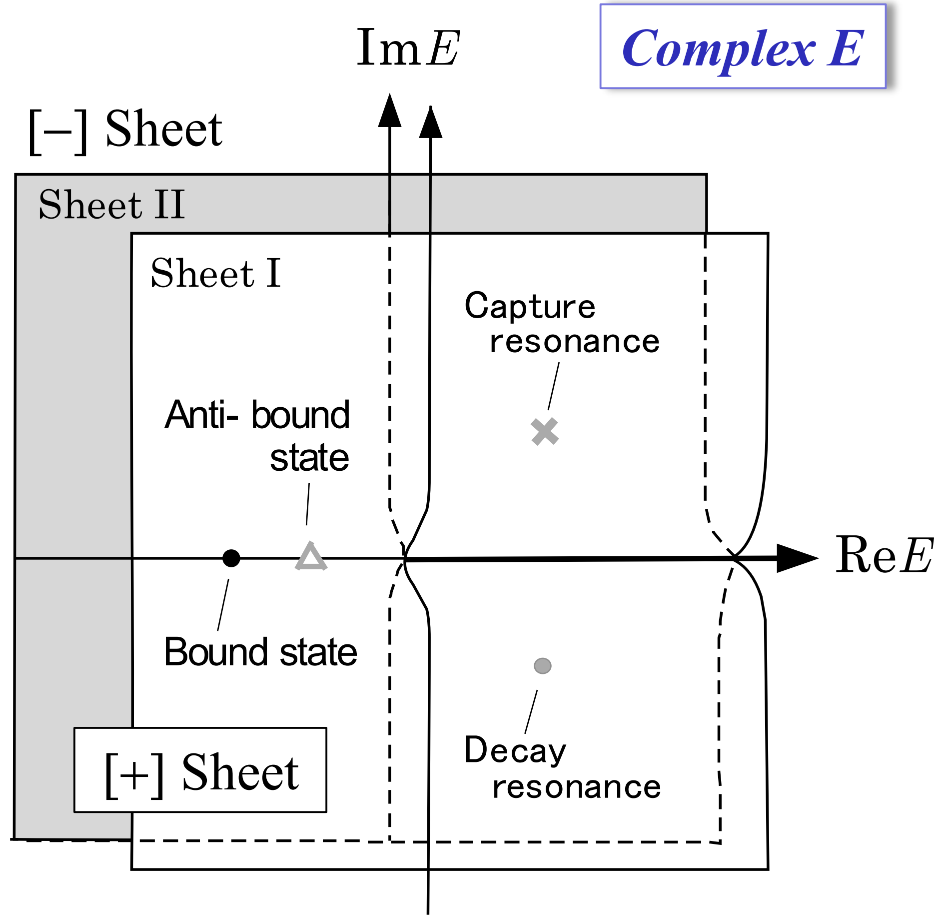

Solving the multichannel Lippmann-Schwinger equation

Lippmann-Schwinger equation

$$|\Psi^{(+)}\rangle = |\phi_{\boldsymbol{k}}\rangle + \frac{1}{E - H_0 + i\varepsilon} U |\Psi^{(+)}\rangle$$

Partial wave expansion

$$R^{\ell}_{\beta\alpha}(k_\beta, r) = k_\alpha r j_\ell(k_\alpha r)\delta_{\beta\alpha} + \sum_\gamma \int_0^\infty dr' g^{(+)}_{\beta,\ell}(k_\beta; r, r') U_{\beta\gamma}(r') R^{\ell}_{\gamma\alpha}(k_\gamma, r')$$

Green's function for β-channel with boundary conditions

[Pearce, Gibson, PRC40(1989)902]
[Miyagawa,Yamamura, PRC60(1999)024003]

$$g^{(+)}_{\beta,\ell}(k_\beta; r, r') = \begin{cases} \dfrac{2\mu_\beta}{\hbar^2}\dfrac{2}{\pi} r r' \displaystyle\int_0^\infty \frac{p^2 j_\ell(pr) j_\ell(pr')}{k_\beta^2 - p^2 + i\varepsilon} dp \\ \dfrac{2\mu_\beta}{\hbar^2}\dfrac{2}{\pi} r r' \left(\displaystyle\int_0^\infty \frac{p^2 j_\ell(pr) j_\ell(pr')}{k_\beta^2 - p^2 + i\varepsilon} dp - 2\pi i \mathrm{Res}|_{p=-k} \right) \end{cases}$$

(+) sheet

(–) sheet

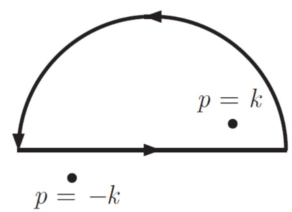

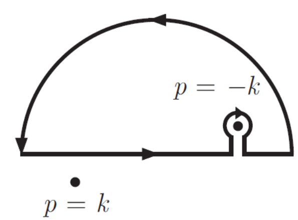

Multichannel T matrix (or S matrix)

$$T^{\ell}_{\beta\alpha}(E) = -\frac{2\mu_\beta}{\hbar^2} \sum_\gamma \int_0^\infty r'^2 dr' j_\ell(k_\beta r') U_{\beta\gamma}(r') \frac{R^{\ell}_{\beta\alpha}(k_\gamma, r')}{k_\gamma r'}$$

Poles of the S-matrix for Σ-2N on 2^4 Riemann Sheets

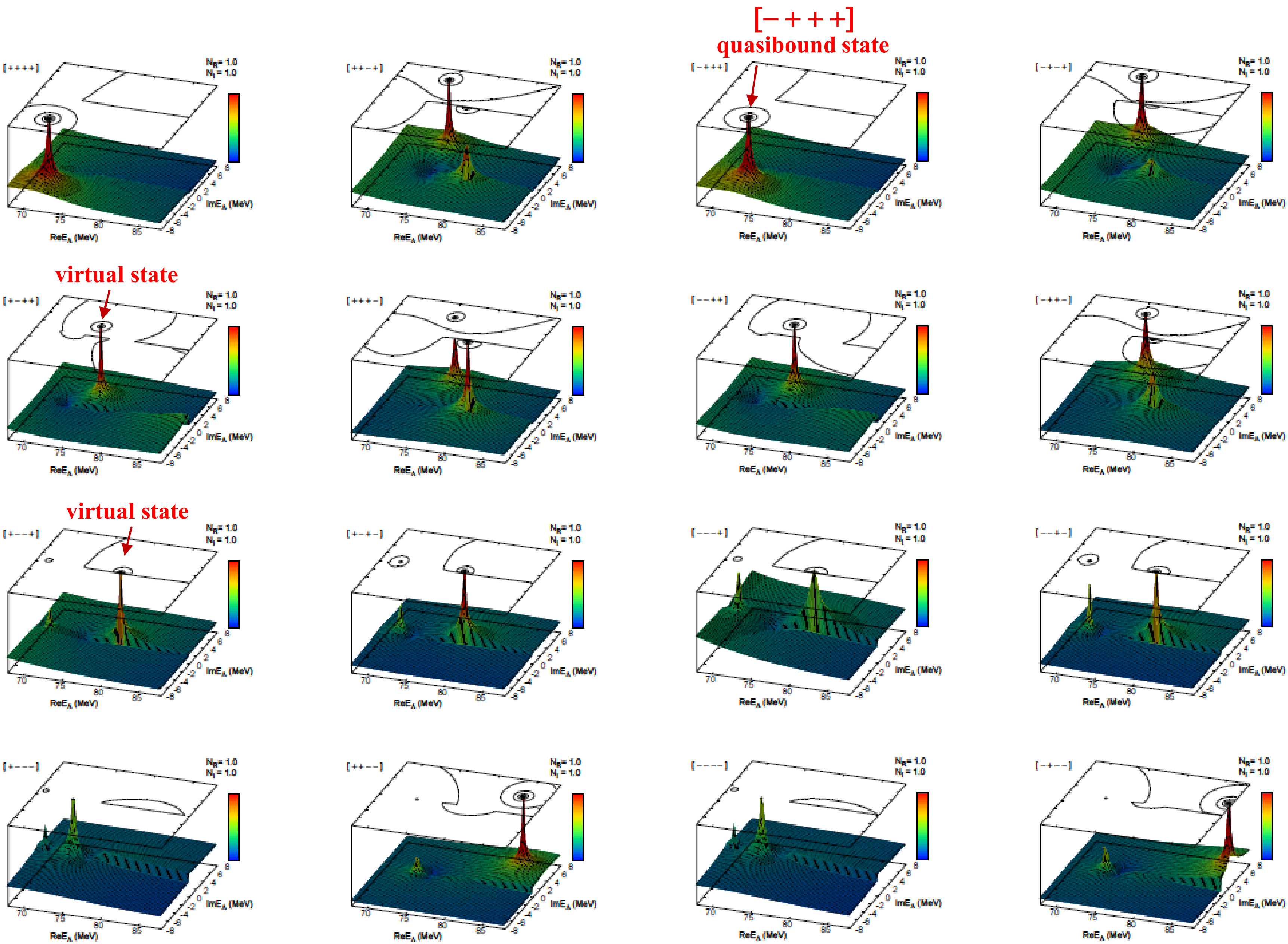

Inclusive spectrum in $^{3}He(K^{-},\pi^{-})$ reactions at 600MeV/c

T.Harada, Y.Hirabayashi, PRC89, 054603 (2014)

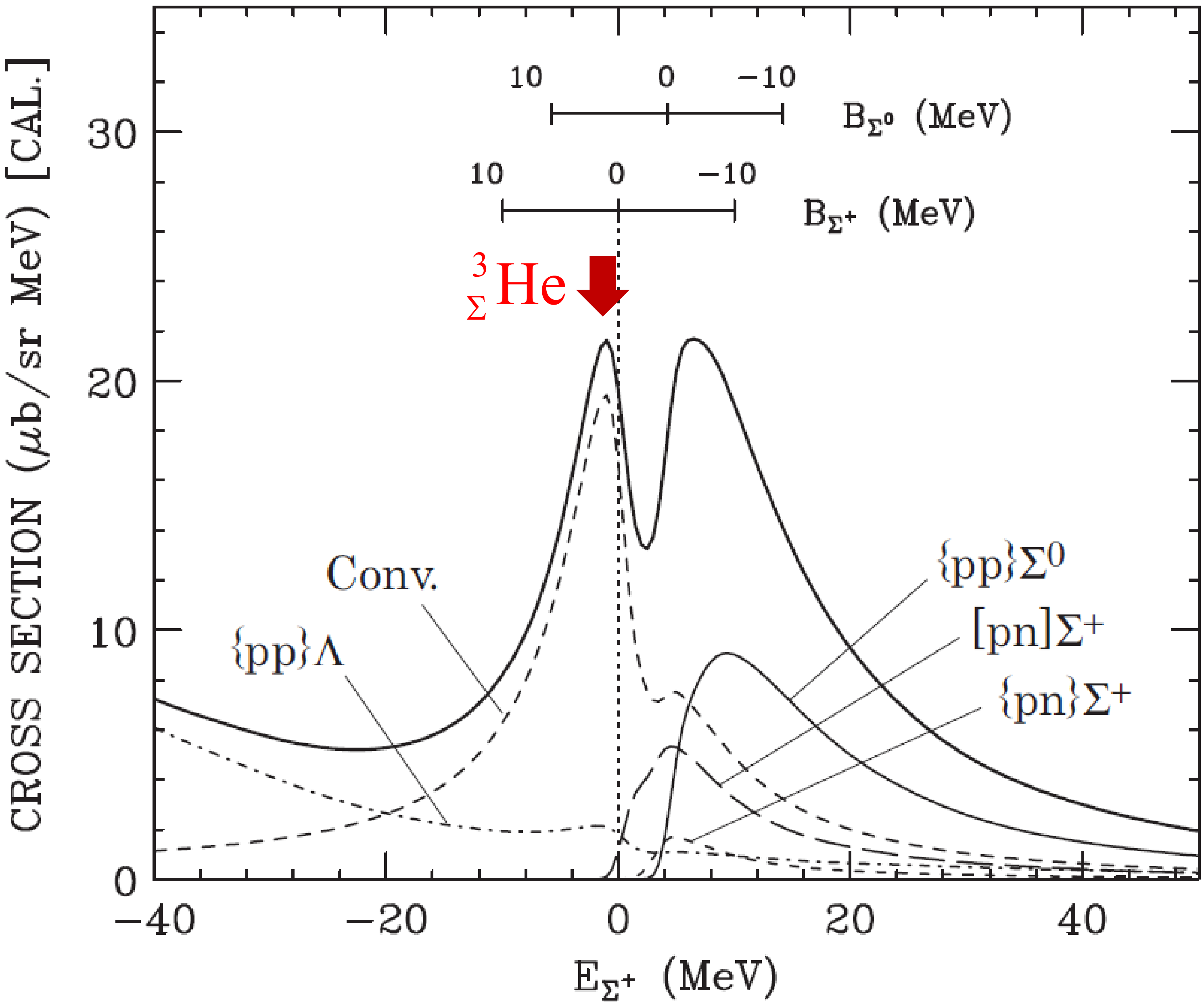

Conparison with the data in ^{3}He(K$^-$,π^+) reactions at 600MeV/c

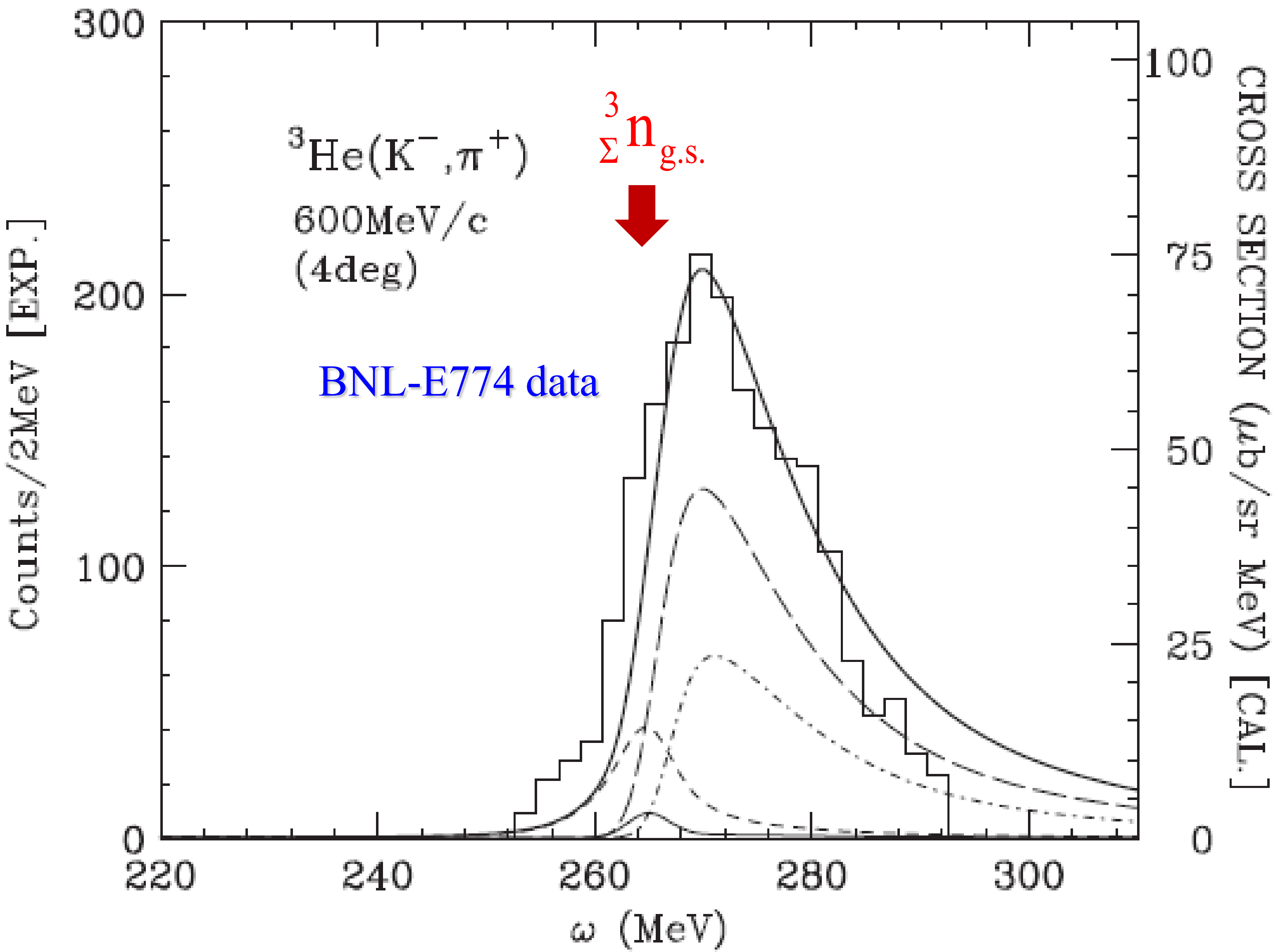

BNL-E774: Barakat, Hungerford, NPA547(1992)157c

Interference between K⁻N-πY amplitudes in the spectra (II)

For ^{3}He(K$^-$,π$^+$) reactions

$$T^{(K^-,\pi^+)} \simeq f_{\Sigma^0}\langle\{nn\}\Sigma^0|^3\text{He}\rangle + f_{\Sigma^-}\langle\{pn\}\Sigma^-|^3\text{He}\rangle + f_{\Sigma^-}\langle[pn]\Sigma^-|^3\text{He}\rangle$$

$$= f_{\Sigma^-}\left(\frac{1}{2}\langle T=2|^3\text{He}\rangle + \frac{1}{2}\langle T=1_s|^3\text{He}\rangle + \sqrt{\frac{3}{2}}\langle T=1_t|^3\text{He}\rangle\right)$$

dynamically admixtures

We assume $\langle T=1^{(-)}| = \frac{1}{\sqrt{2}}\langle T=1_s| - \frac{1}{\sqrt{2}}\langle T=1_t|$, but it depends on (2N)-Y pot.

$$= f_{\Sigma^-}\left(\frac{1}{2}\langle T=2|^3\text{He}\rangle + \frac{2\sqrt{3}-\sqrt{2}}{4}\langle T=1^{(-)}|^3\text{He}\rangle\right.$$

$^3_\Sigma$n$_{g.s.}$ most attractive

Reduced 0.51

Enhanced

$$\left. + \frac{2\sqrt{3}+\sqrt{2}}{4}\langle T=1^{(+)}|^3\text{He}\rangle\right)$$

$^3_\Sigma$n*

1.219

➢ **This reduction mechanism must appear in ^{3}He(K$^-$,π$^+$) reactions !**

Remarks

- There is a quasibound in ΣNN systems with $J^p = 1/2^+$, L = 0, S = 1/2 state. ${}^{3}_{\Sigma}\mathrm{He}$, ${}^{3}_{\Sigma}\mathrm{H}$, ${}^{3}_{\Sigma}\mathrm{n}$

- The pole is located as

$$\mathcal{E}^{(\mathrm{pole})}_{\Sigma^+}({}^{3}_{\Sigma}\mathrm{He}) = +0.96 - i\,4.5\ \mathrm{MeV} \qquad (K^-, \pi^-)$$

$$\mathcal{E}^{(\mathrm{pole})}_{\Sigma^0}({}^{3}_{\Sigma}n) = -0.58 - i\,5.3\ \mathrm{MeV} \qquad (K^-, \pi^+)$$

measured from the $d + \Sigma^+$ threshold .

- The pole positions reside on the second Riemann sheet [− + + +] on the complex E plane.

$$[\mathrm{Im}k_{\{pp\}\Lambda},\ \mathrm{Im}k_{[pn]\Sigma+},\ \mathrm{Im}k_{\{pn\}\Sigma+},\ \mathrm{Im}k_{\{nn\}\Sigma0}\ ]$$

5. ^{3}He(K^{-}, π^{-}) *ppΛ* reactions by CDCC method

T. Harada, Y. Hirabayashi, NPA934 (2015) 8.

Continuum Discretized Coupled Channel method (CDCC)

M. Kamimura et al., PTP. Suppl. 89, 1 (1986)

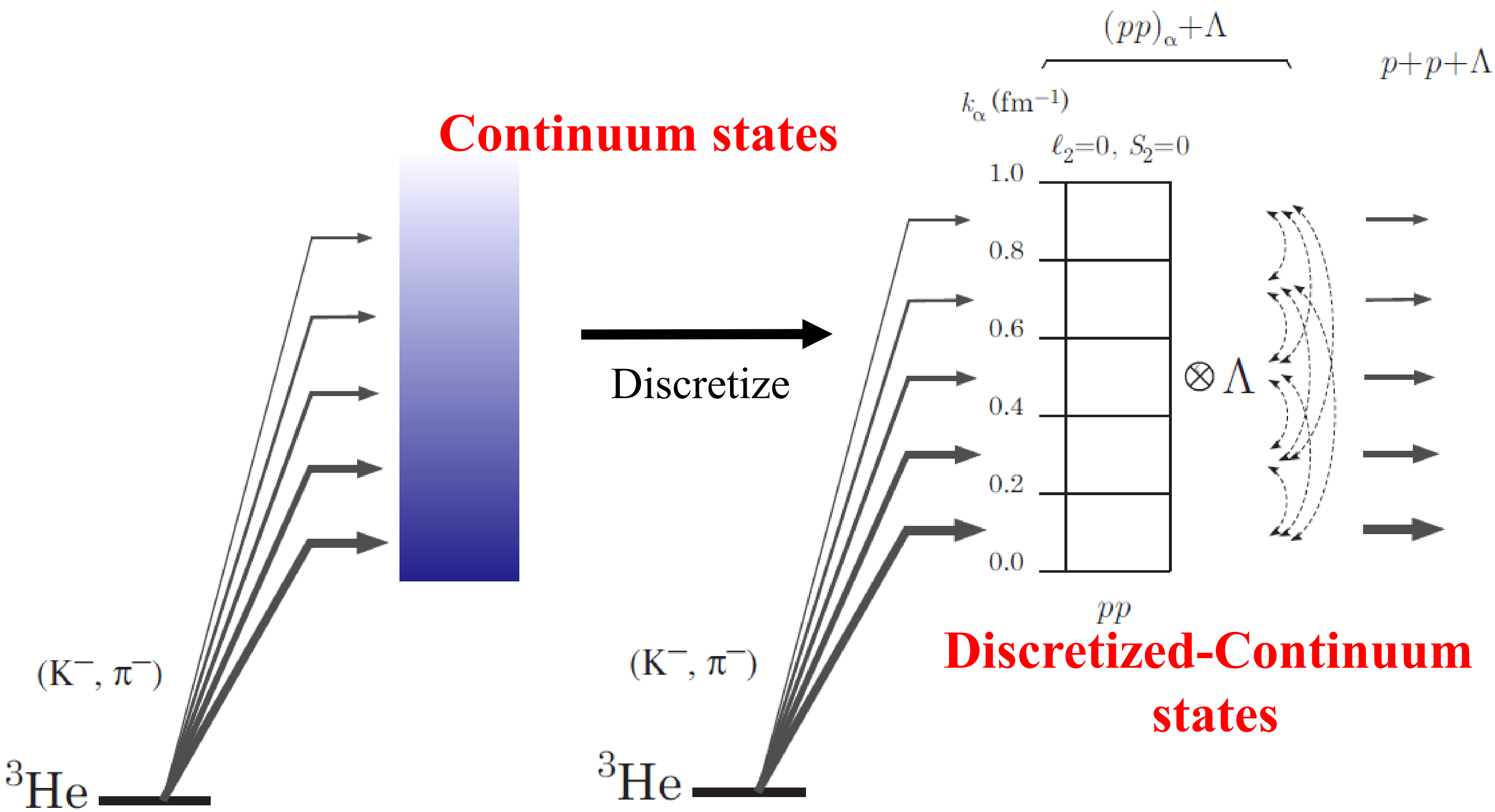

Inclusive spectrum in $^3He(K^-,\pi^-)pp\Lambda$ at 870MeV/c

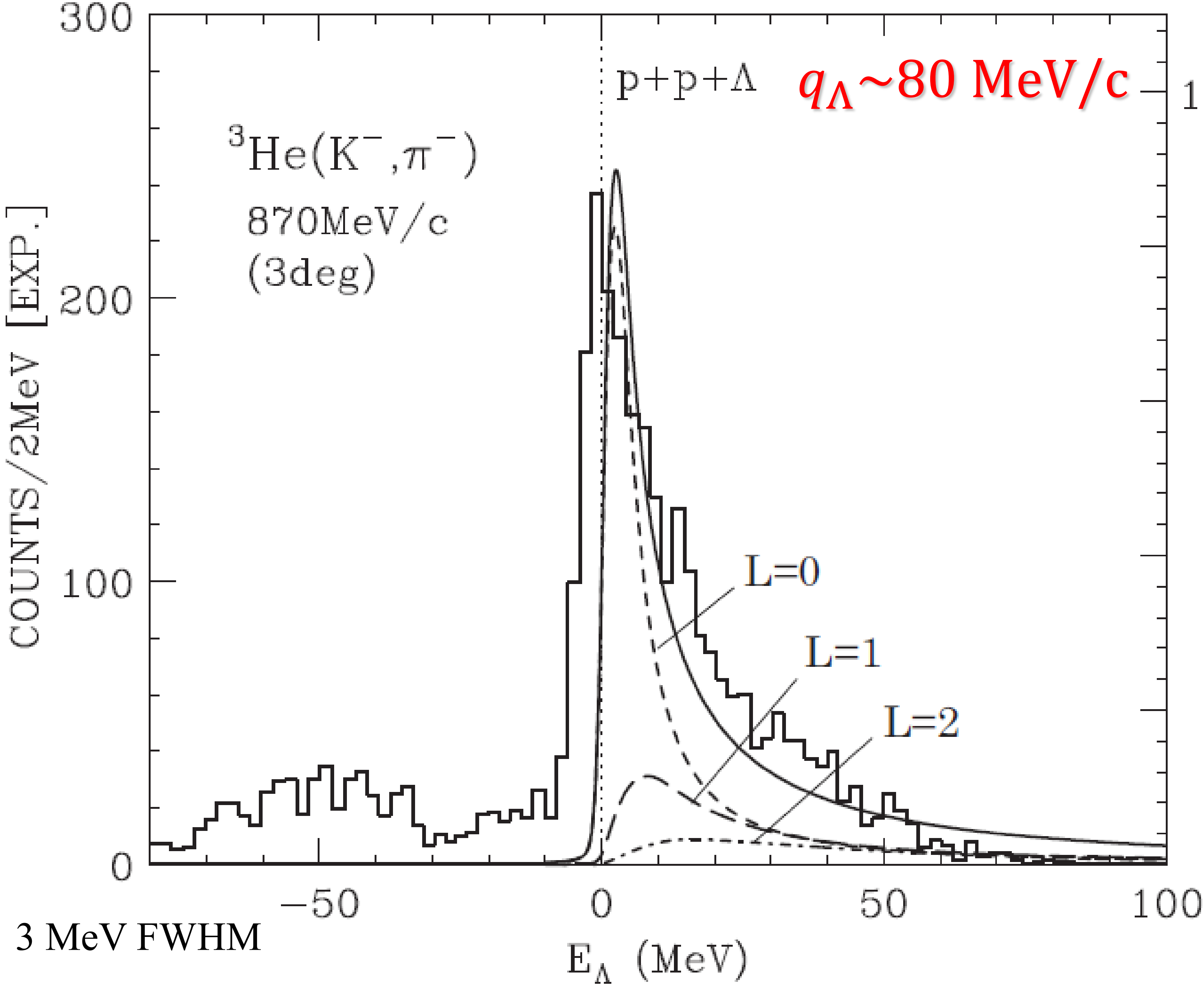

3 MeV FWHM

Inclusive spectrum in ^{3}He(K^-,π^-)ppΛ at 870MeV/c

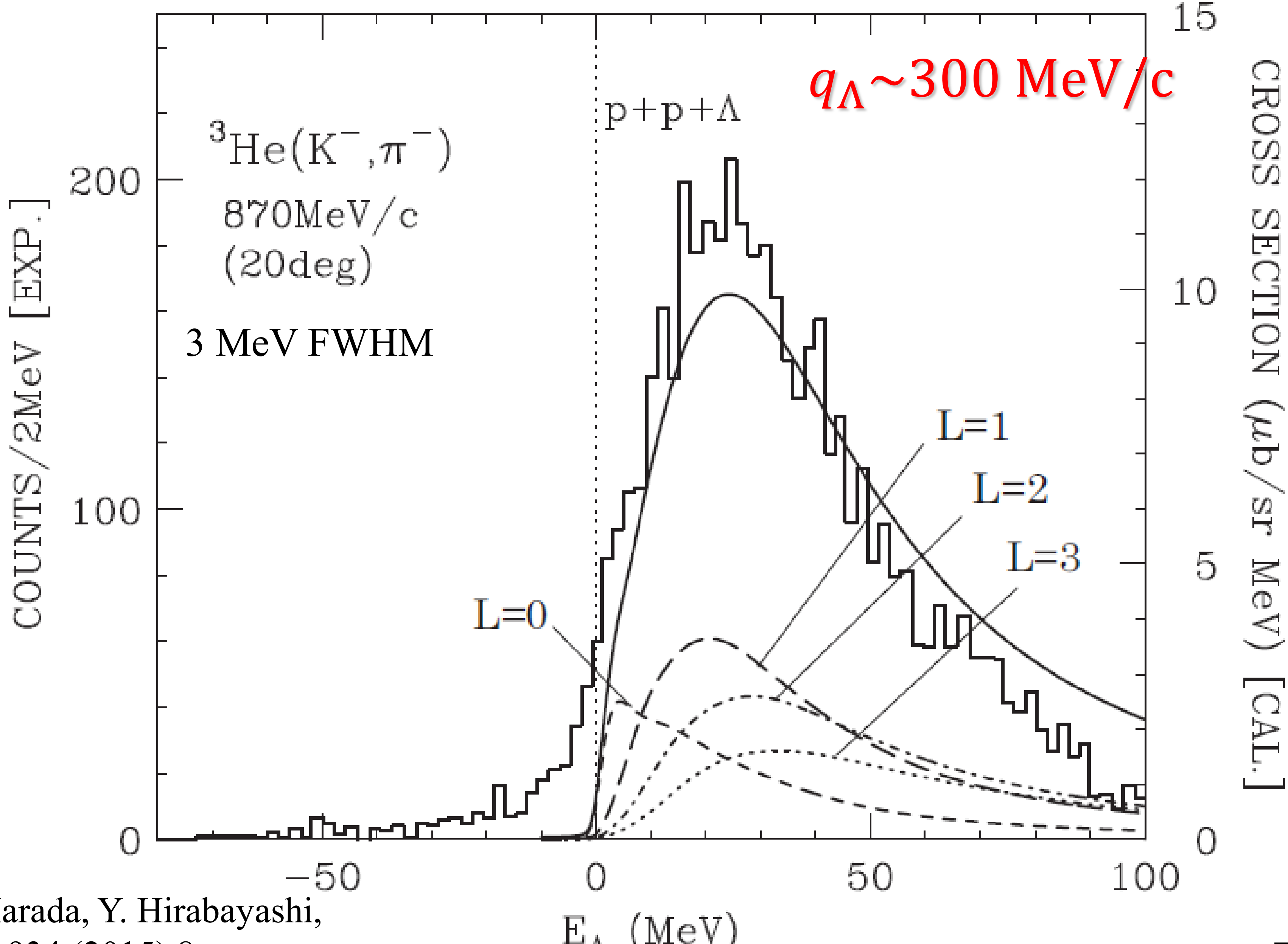

T. Harada, Y. Hirabayashi,
NPA934 (2015) 8.

Remarks

- The coupled-channel framework is very important for calculating the spectra of the ^{3}He(K$^-$,$\pi^\mp$) reactions.
  taking into account K$^-$N-πY amplitudes and threshold-differences .
- The effective "2N"-Y potential is constructed from the MS theory with correlation functions.
  More detailed investigations are needed. ←→ Full 3B calculations
- Both the π^- and π^+ spectra provide valuable information to understand the nature of the ΣNN quasistates and also the YN (ΣN) interactions.
  To determine a quasibound state [+ −] or cusp state [− +].
- It is easy to apply this framework to the CDCC in order to take into account the nuclear breakup processes in continuum states. Considering the ppΛ spectra via ^{3}He(K-,π-) reactions.

6. DCX productions via (π^-, K^+) and (K^-, K^+) reactions

Harada, Hirabayashi, PRC105 (2022) 064606.

7. Extended optimal Fermi averaging

Harada, Hirabayashi, PRC105 (2022) 064606.

微視的チャネル結合(MCC)法

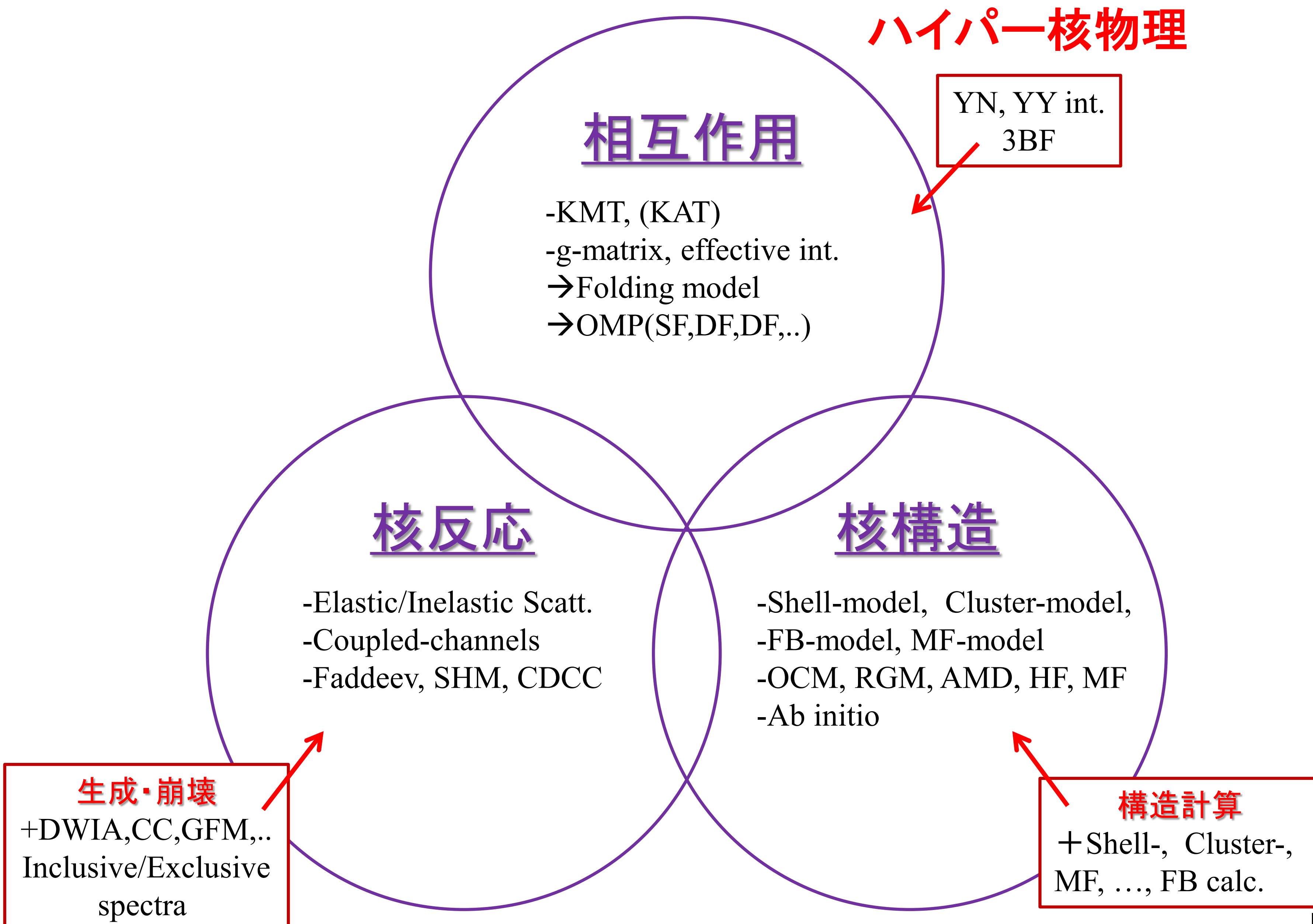

Summary

- Distorted wave impulse approximation (DWIA)
- Ξ-nucleus potentials studied by (K^-, K^+) reactions
- $^{3,4}_{\Lambda}$H productions for $^{3}_{\Lambda}$H lifetime puzzle
- Search for a ΣNN quasibound state
- ^{3}He(K$^-$, π$^-$) $pp\Lambda$ reactions by CDCC method

- DCX productions via (π^-, K^+), (K^-, K^+) reactions
- Extended Optimal Fermi averaging (EOFA)
- ….

Thank you very much.